

Optimization approach of berth-quay crane-truck allocation by the tide, environment and uncertainty factors based on chaos quantum adaptive seagull optimization algorithm



Ming-Wei Li ^{a,b}, Rui-Zhe Xu ^{a,b}, Zhong-Yi Yang ^c, Wei-Chiang Hong ^{d,e,*}, Xiao-Gang An ^{a,f}, Yi-Hsuan Yeh ^d

^a College of Shipbuilding Engineering, Harbin Engineering University, Harbin 150001, China

^b Nanhui Institute, Harbin Engineering University, Sanya 572024, Hainan, China

^c School of Economics and Management, Harbin Engineering University, Harbin 150001, China

^d Department of Information Management, Asia Eastern University of Science and Technology, New Taipei 22046, Taiwan

^e Department of Information Management, Yuan Ze University, Zhongli 320315, Taiwan

^f China Waterborne Transport Research Institute, Beijing 100088, China

HIGHLIGHTS

- TEU-BQCT model is proposed to optimize berth-quay crane-truck allocation.
- CQASOA is proposed to improve the global perturbation and convergence ability of the algorithm.
- This paper applies TEU-BQCT_CQASOA approach to receive appropriate distribution plan of port size.

ARTICLE INFO

Keywords:

Berth-quay crane-truck joint scheduling
Tidal factor
Uncertainty factor
Seagull optimization algorithm
External penalty function method
Quantum computing
Chaotic mapping

ABSTRACT

The post-epidemic era has led to the accumulation of cargo, which has brought greater pressure to container ports. Since traditional methods cannot simultaneously consider the effect of tidal, uncertain, and environmental factors on the allocation plan. To relieve this pressure, firstly, considering tidal factors, formulating time window rules, thinking out uncertain factors, and determining constraints from three perspectives of vessel berthing process, quay crane and container truck operation, a new berth-quay crane-truck joint scheduling model is constructed by minimizing three aspects of vessels turnaround time, the carbon emissions of quay cranes and trucks, namely TEU-BQCT model. Then, aiming at obtaining a relatively high-quality solution, combining chaotic mapping and quantum entanglement, a new chaotic quantum adaptive seagull optimization algorithm is proposed, namely CQASOA, exclusive coding rules suitable for the TEU-BQCT model is formulated, a feasible integer algorithm is developed, the external penalty function is constructed to limit constraints, and a novel joint scheduling solution method of berth-quay crane-truck is proposed, namely TEU-BQCT_CQASOA. Subsequently, two ports of different scales in South China are used to test the constructed solution method feasibility. The simulation results indicate that the constructed TEU-BQCT model can obtain a more suitable scheduling scheme. The proposed CQASOA has better performance than other comparison algorithms selected in this paper, which can obtain a better solution when solving the TEU-BQCT model.

1. Introduction

The continuation of the new crown epidemic has seriously affected the global economy and trade, causing a great impact on the global supply and demand sides. As an important mode of transportation in

international trade, shipping has been more seriously affected [1]. In 2021, the average waiting time of vessels at Los Angeles Port in the US, Felixstowe Port in the UK, Rotterdam Port in the Netherlands, and Piraeus Port in Greece will reach 16.5, 13.8, 8.8, and 9.1 days respectively. Compared with 2020, it is still rising in the same period, and the

* Corresponding author at: Department of Information Management, Asia Eastern University of Science and Technology, New Taipei 22046, Taiwan.
E-mail address: samuelsonhong@gmail.com (W.-C. Hong).

congestion situation is still very serious [2]. In addition, green and low carbon has become the theme of the era, and governments around the world are advocating to control port energy consumption in a green and clean way. Therefore, this paper focuses on providing port managers with a scheduling solution to solve the problem of congestion and carbon emissions in the post-epidemic era of ports.

Container port logistics scheduling has the characteristics of multiple links and processes. In the scheduling process, there are more influencing factors. It is necessary to consider the influence of uncertainties such as tides, meteorology and man-made on port scheduling. Specifically, the main contributions of this article are as follows:

a) Considering tidal factors, formulating time window rules, thinking out uncertainties such as meteorological and man-made factors, and determining constraints from three perspectives of the vessel berthing process, quay crane and truck, a new optimal model for berth-quay crane-truck allocation, namely TEU-BQCT, is proposed, by taking the minimize three aspects of vessels turnaround time, the carbon emissions of quay cranes and trucks as the optimization objectives.

b) Given insufficient diversity and easy stuck in local optimum in the SOA evolution later stage, a novel chaotic quantum adaptive seagull optimization algorithm, namely CQASOA, is proposed, with a population initialization method based on chaotic mapping (CSOA) is established to increase the ergodicity of the initial population; A quantum revolving gate and quantum NOT gate using quantum computing (QSOA) is proposed to enhance the population convergence speed; An adaptive weight factor (ASOA) is introduced to enhance the global disturbance capability in the SOA early stage and the local search capability in the later stage.

c) This paper, based on the CQASOA and the TEU-BQCT model, formulates the individual coding rules, designs the feasible-integer processing algorithm (F-IP), constructs external penalty functions to limit constraints and establishes a novel berth-quay crane-truck allocation approach, namely TEU-BQCT_CQASOA, which can offer different distribution plan according to different operation requirements by adjusting the weight of sub-objective function and can get a more appropriate distribution plan with the growth of port size.

The rest of this article is organized as follows: The existing work and contributions are contained in Section 2; Section 3 describes the TEU-BQCT model; Section 4 introduces the proposal of CQASOA and the establishment of the solution method of TEU-BQCT_CQASOA; The data experiment and simulation research is present, and the performance of the model and algorithm proposed is analyzed in Section 5; Section 6 concludes this paper.

2. Literature review

2.1. Optimization of container port logistics joint scheduling

Container port loading and unloading operations have many links and complex processes, and there are still some difficulties in providing a scheduling scheme that controls the whole port [5]. To avoid too ideal scheduling results, more and more scholars have researched joint scheduling of container port loading and unloading operations [6–11]. Liu et al. [12] constructed a new berth and quay crane joint scheduling in response to the unfair distribution of quay cranes. Ma et al. [13] aimed at improving the utilization rate and service quality of quay cranes and establishes a joint dispatch planning model which can minimize the vessel service cost during the planning period. Gao et al. [14] established a mathematical model to improve the utilization rate of container port equipment and decrease the vessel working time in ports. Yu, et al. [15] considered the difference in ship services and proposed a cooperative mode of vessel speed optimization and joint berth-quay crane allocation. The simulation results reveal that the method can enhance customer satisfaction and decrease carbon emissions. Liu et al. [16] investigated joint berth allocation and quay crane assignment problem considering uncertain arrival time of vessels and operation efficiency of quay cranes. The authors of this paper have also made research work in related fields. Li et al. [17] established a multi-objective joint allocation model which can reduce the transportation distance of the truck and decrease vessels' turnaround time. Simulation examples show that this method can provide solutions for container ports. Cao et al. [18] constructed a joint allocation model

Table 1
Existing work summary sheet.

Reference	Objective	Model	Problem solved
Liu et al.[12]	Min port time Min system cost Min unfairness	A multi-objective scheduling model	Solve the unfair distribution of berths and quay cranes
Ma et al.[13]	Min the arriving vessel service cost	A berths and quayside cranes scheduling model	Obtain berth and quayside crane resources method and enhance service quality
Gao et al.[14]	Min total vessel time in port	The mathematical optimization model of BACAP	Cut down the vessel time in port and improve equipment utilization
Yu, et al.[15]	Min vessel fuel costs Min service delays of vessels Min vessel service delays	A bi-level multi-objective optimization model	Cut down fuel consumption costs of vessels, service delays, and improve customer satisfaction
Liu et al.[16]	Min the vessel delayed departure time Min the total berth deviation Min the total operation cost of quayside cranes	A joint dispatch model for berth-quay crane	Cope with complex situations of the quayside operation
Azab et al.[19]	Min the number of relocations	A container trucks relocation scheduling model	Raise container relocation operations at terminal yards
Essghaier et al. [20]	Min the total delay Min the sum of PI-containers traveled distances	A Multi-Objective Mixed-Integer Programming model	Generate a robust Pareto front that aligns with decision-makers' attitudes towards risk
Duan et al.[21]	Min the average waiting time Min vessel departure delay	A joint dispatch model for berth-quay crane	Obtain a more green and reasonable solution for the berths and quayside cranes operation
Wang et al.[22]	Min port carbon emissions	A joint dispatch model for berth-quay crane	Improve port handling efficiency and reduce carbon emissions
Kenan et al. [23]	Min the berthing time of vessels Min port carbon emissions	A joint dispatch model for berth-quay crane	Improve port handling efficiency and reduce carbon emissions
This study	Min time of vessels in port Min truck carbon emissions Min quay crane carbon emissions	A novel berth-quay crane-truck joint scheduling model	Consider tides, environment, and uncertainties, cut down the port's carbon emission and meet the needs of the port during the epidemic

considering economic factors and solved it with the improved sparrow algorithm. Simulation examples show that the scheduling method can reduce the cost of ports.

Some good solutions for the berth-quay crane joint dispatch are provided by the above research work, which can decrease the container port cost and enhance the utilization rate of container ports. However, the components of port dispatch operations affect each other. The quay crane's working efficiency is limited by the number of trucks and is also affected by the scheduling of trucks at the front of the terminal. Therefore, in the land operation scheduling process, it is still necessary to comprehensively consider the impact of trucks on the distribution of berths and quay cranes. Azab et al. [19] proposed two binary IP models to solve the new optimization problem and results show that the proposed approach can improve container relocation operations at terminal yards by coordinating with appointment scheduling. Essghaier et al. [20] established a Multi-Objective Mixed-Integer Programming model (FMO-MIP) that incorporates fuzzy chance-constrained programming and ϵ -constraint to minimize both the total delay and the sum of PI-containers traveled distances, while considering the uncertainty on truck arrival times. However, there are still few joint dispatches of berths, quay cranes and trucks in the existing literature, whose modeling and solution methods still need to be further explored.

The topic of environmental protection has attracted the attention of various countries to climate change, and the issue of carbon emissions in container ports has also become a current research hotspot. Duan et al. [21] constructed a mathematical model for the rational utilization of container port resources and the reduction of carbon emissions. Taking Ningbo Port as an example, the author evaluated the impact of carbon emission cost changes on the berth and quay crane distribution scheme and proposed a solution. Wang et al. [22] established a planning model for the willingness of container ports to reduce carbon emissions under the new carbon tax policy, provided solutions, assessed the impact of carbon emissions tax on carbon emission reduction, and reduced the carbon emissions of container ports. Kenan et al. [23] established a mathematical model, integrated the allocation and scheduling of dock cranes, and considered the carbon regulatory policy, which can cut down the berthing time and carbon emissions from vessels. However, the existing models cannot adapt to the current post-epidemic era background, and the port machinery collaborative work needs further research, the above research work is summarized as shown in Table 1. Therefore, in Section 3, a novel berth-quay crane-truck joint scheduling model that considers the tide, environment, and uncertainty factors will be proposed to make a dispatching scheme more in line with the era background for port decision-makers.

2.2. Algorithm for joint logistics scheduling planning model of container ports

The solution problem of the joint scheduling planning model of container port logistics has the characteristics of multiple and nonlinear, and cannot be solved precisely. The usual method is to approach the extreme point through the solution algorithm. Tian et al. [24] built a mathematical model intending to cut down the total logistics operation cost and solved it by using the linear programming method and the commercial software ILOG CPLEX. Cheimanoff. et al. [25] proposed a new Mixed Integer Linear Formulation (MILP) and Variable Neighbor Search (VNS) method to solve the quay crane allocation model. In the wake of the increase in computing power, the intelligent optimization algorithm is also widely used and performs well in solving this type of optimization problem [26–28]. Skaf et al. [29] established a planning model for the scheduling problem of multiple-yard trucks and a single quayside crane, using the genetic algorithm to solve the model. Chu et al. [30] proposed a comprehensive container liner route planning and speed scheduling method, which was solved based on the genetic algorithm.

With the improvement of computer computing power, more and

more high-quality optimization algorithms have been proposed, which have been proved to be successful in various applications, such as experiment-based approach to teach optimization techniques [31], neural network-based control using actor-critic reinforcement learning and gray wolf optimizer with experimental servo system validation [32], marine predator inspired naked mole-rat algorithm for global optimization [33]. Considering the excellent performance of SOA algorithms in container port scheduling, SOA is tried to solve such models [4]. However, SOA has problems such as being easily stuck in local optimum and slow convergence speed. Ewees et al. [34] use Lévy flight and mutation operators for SOA linear search spaces, improving the exploration-mining trade-off to quickly and accurately capture optimal solutions. Ma et al. [35] aimed at the shortcomings of SOA with low convergence accuracy, weak overall diversity, and tendency to local optimum, proposed CMSOA, and the statistical calculation proved that the proposed algorithm has advantages. Xiao et al. [36] used opposition-based learning (OBL), Cauchy distribution, and inverse sigmoid functions to enhance SOA based on Dual-Hidden-Layer Extreme Learning Machine (TELM) with Hyperparameter Activation Functions, and the calculation results show well. Xu et al. [37] combined the mechanism of natural selection based on SOA and found the optimal solution by sorting the population using fitness values to replace the worst half with the best half.

The study done in the existing method can improve the optimization performance of SOA, but when solving complex problems, it still exposes deficiencies in global perturbation capability and computing performance. The authors have tried to improve the intelligent optimization algorithm by chaotic disturbance and quantum entanglement, and proposed the novel chaotic bat algorithm [38], chaos adaptive genetic algorithm [39], cat mapping, cloud model and PSO hybrid algorithm [40], the chaotic cloud particle swarm optimization [41], chaos cloud quantum bat hybrid optimization algorithm [42], quantum butterfly optimization algorithm [43], hybrid genetic cloud whale optimization algorithm [44] to solve the problem of optimization. Experiments verified that the above-improved algorithms had achieved good results. The above improvement methods can provide a good reference for this article. Therefore, aiming at the defects of SOA, a new chaotic quantum adaptive seagull optimization algorithm is proposed by combining chaotic mapping and quantum computing, namely CQASOA, to enhance the optimization performance of the algorithm.

3. Establishment of TEU-BQCT model

Considering that large vessels need to use the tidal water level to enter the port, the water level time window rules are formulated according to the draft depth and periodic timetable of large vessels. If the water level in a certain period meets the needs of large vessels entering the port, the water level in this period is the high water level time window. Conversely, it is the low water level time window. The periodic change of the tide makes the high and low water level time windows appear alternately. This paper assumes that the traversal times of the high and low water level time windows are approximately equal.

Considering the robustness of improving the construction model, this paper introduces uncertainty factors. When the vessel sails into the port, the expected arrival time of the container port will be provided. Due to climate and human factors, the actual vessel arrival time may change. The deviation time obeys the Erlang distribution law [45], which is determined based on the statistical law of the port. In addition, due to human factors, the deviation of the operating speed of the truck is considered to obey the normal distribution law which is determined according to the statistical law of container trucks.

In the scheduling optimization process, we divide the continuous shoreline into several discrete berths. Duplicate or cross-berth berthing is not allowed during the berthing process. Also, the vessel is only permitted to complete one operation. Each quayside crane can only serve one vessel at a time. The minimum vessel time in port and the

carbon emissions from trucks and quay cranes should be the guideline to determine the order of berthing and the allocation of berths, quay cranes, and trucks.

3.1. Assumptions and notations

The assumptions of the TEU-BQCT model are established from three aspects: berths, quay cranes, and trucks. The details are as follows:

(1) It is assumed that the vessel provides the estimated time for arriving at the port, but due to the environmental interference, the actual vessel arrival time has a deviation time which follows the Erlang distribution;

(2) Considering the influence of tidal factors on vessels entering and leaving the port, large vessels are only permitted to sail into the port at the tidal level, and the time for each vessel to enter and exit the channel is equal and a fixed constant;

(3) It is assumed that the length of each water level time window is equal;

(4) A continuous berth line is divided into discrete berths whose length, width, and water depth meet the requirements of the vessel;

(5) Each vessel is only allowed to berth once and the berth cannot be moved after berthing;

(6) After the vessel starts operations, the assigned quay crane work efficiency remains unchanged;

(7) The upper and lower limits of the quay crane allocation meet the requirements of vessel working restrictions;

(8) It is assumed that the quay crane can be moved to the adjacent berth when it is idle, but the quay crane is not permitted to step over other quay cranes;

(9) Considering that the driving speed of the truck is disturbed by artificial uncertain factors, it obeys the normal distribution law;

(10) It is assumed that the number of cranes in the container yard is sufficient and the loading and unloading efficiency remains unchanged.

The TEU-BQCT model application parameters are categorized by Sets, Optimization variables, Input Parameters, Dependent Variables, and 0–1 Decision Variables as follows:

Sets:

VVessel, $V = [1, 2, \dots, v]$;

BBerth, $B = [1, 2, \dots, b]$;

CCrane, $C = [1, 2, \dots, c]$;

TTime, $T = [1, 2, \dots, t]$;

YTruck, $Y = [1, 2, \dots, y]$;

V^LA set of large vessels arriving at the port;

VOA set of the order of vessels sailing into the port;

VBA set of the serial number of the berth to be parked;

VC A set of the serial number of allocated quayside cranes for vessel operations;

CK A set of the number of service quayside crane collection trucks;

VKA set of the number of vessel operation trucks;

Optimization variables.

VO_iVessel i berthing sequence;

$$u_{iu} = \begin{cases} 1 & \text{if vessel } i \text{ sails into the channel in the } u\text{-th high water time window} \\ 0 & \text{else} \end{cases}$$

$$v_{iu} = \begin{cases} 1 & \text{if vessel } i \text{ sails out of the channel in the } u\text{-th high water time window} \\ 0 & \text{else} \end{cases}$$

VB_iThe berth of the vessel i ;

VC_iThe number of quay cranes serving vessels i .

VK_iThe number of trucks distributed for the operation of vessel i ;

Input Parameters:

WTThe length of each high/low water level time window;

RSufficiently large integer;

MContainer ports have the total number of available collection trucks;

TO_iVessel i estimated time of arrival;

TG₀The travel time required for a vessel to pass through the channel.

CE_iThe theoretical work efficiency of a single quayside crane;

CF₀The theoretical work efficiency of a single crane in the container yard;

TW₀The maximum waiting time of vessels;;

VL_iThe length of vessel i ;

VD_iThe draft of vessel i ;

VE_iThe number of containers carried by vessel i ;

BL_jThe length of berth j ;

BD_jThe draft of berth j ;

D_{ij}The distance between the vessel i docked at berth j and the target yard;

VC_{mi}The lower limit of quay cranes serving vessel i ;

VCM_iThe upper limit of quay cranes serving vessel i ;

Dependent Variables:

TA_iThe vessel i actual arrival time;

TB_iThe start time of sailing into the channel for vessel i ;

TC_iThe time when the vessel i entered the port;

TS_iVessel i loading and unloading operation start time;

TD_iVessel i loading and unloading operation end time;

TV_iThe start time of the adjacent quay crane executing operation for the vessel i ;

TE_iThe start time of vessel i sailing out of the channel when leave the port;

TF_iThe time for vessel i sailing out of the port;

TH_{ij}The time spent by vessel i at berth j for empty transport of trucks;

TL_{ij}The time takes for vessel i to dock at the berth j for the heavy-load transportation of trucks;

VC_{it}The number of quay cranes serving vessel i at time t ;

CK_{nt}The number of trucks serving quay crane n at time t ;

CE_tThe actual work efficiency of a single quayside crane;

D_tThe total mileage of trucks under heavy load;

D_kThe total mileage of trucks with no load;

t_pThe total idle time of trucks;

v_tThe speed of the container truck when it is not loaded;

v_oThe speed when the container truck is overloaded;

0–1 Decision Variables:

$$x_{ijk} = \begin{cases} 1 & \text{if vessel } i \text{ served according to sequence } k \text{ at berth } j \\ 0 & \text{else} \end{cases}$$

$$q_{in} = \begin{cases} 1 & \text{if quay crane } n \text{ serves for vessel } i \text{ within time } t \\ 0 & \text{else} \end{cases}$$

3.2. Objective function F

Aiming at achieving the best balance between port benefits, ship-owner interests, and environmental protection, the economic benefits

and environmental factors of container ports are considered comprehensively, and the optimization model is constructed with the minimum vessels turnaround time, the minimum carbon emissions of trucks, and the minimum carbon emissions of quay cranes as objective functions. The objective function of the TEU-BQCT model can be expressed by Eq. (1),

$$F = \min(\omega_1 \cdot k_1 \cdot F_1 + \omega_2 \cdot k_2 \cdot F_2 + \omega_3 \cdot k_3 \cdot F_3) \quad (1)$$

where F is the objective function; F_1 , F_2 , F_3 are three sub-objective functions; ω_1 , ω_2 , and ω_3 are the weight adjustment factors; k_1 , k_2 , and k_3 are the magnitude balance coefficients.

It is the most ideal state that vessels' turnaround time and the carbon emissions of the port should be minimized at the same time, but there are mutual constraints among various indicators, and even there is a trade-off between them. For instance, reducing the waiting time of vessels in port requires improving operational efficiency, which will inevitably bring about more environmental pollution. Therefore, in the process of formulating the scheduling plan, it is necessary to pay special attention to a certain indicator according to the different needs of different periods. Thence, this paper applies the linear weighting method which can solve the multi-objective optimization problem. Then, the weight adjustment factors ω_1 , ω_2 , and ω_3 are introduced to satisfy the different demands of the port in distinct periods through human intervention as shown in Eq. (2),

$$\omega_1 + \omega_2 + \omega_3 = 1 \quad (2)$$

In addition, the magnitude balance coefficients k_1 , k_2 , and k_3 are introduced to ensure that the influence weights of each sub-objective function are equal. The magnitude balance coefficient can be determined by the magnitude of the objective function value of a specific calculation example. Recommended values are: $k_1 = 1000$, $k_2 = 1$ and $k_3 = 1$.

3.2.1. Sub-objective function F_1

This paper considers the comprehensive benefits of shipowners and container ports and takes the minimum time of vessels in port as the first sub-objective function of the TEU-BQCT model to lessen the waiting time of shipowners in port and raise the work operation efficiency of the port. The sub-objective function F_1 of the TEU-BQCT model is determined as Eq. (3),

$$F_1 = \frac{1}{v} \left[\sum_{i=1}^v (TF_i - TA_i) \right] \quad (3)$$

where F_1 is the first sub-objective function(h); TF_i is the departure time of vessel i ; TA_i is the actual arrival time of vessel i .

3.2.2. Sub-objective function F_2

The operation of a container port should not only ensure economic benefits but also promise environmental friendliness. The minimum carbon emissions of trucks are identified as the second sub-objective function of the TEU-BQCT model to reduce the carbon emissions and the truck fuel consumption of container ports, indirectly controlling the cost of trucking operations. The sub-objective function F_2 of the TEU-BQCT model consists of three parts: the carbon emissions of trucks in no-load driving, the carbon emissions of trucks in heavy-duty driving, and the carbon emissions of trucks in idling speed, which can be defined by Eq. (4):

$$F_2 = E_1 (\rho_l \cdot D_l + \rho_k \cdot D_k + \eta \cdot t_\eta) \quad (4)$$

where F_2 is the second sub-objective function (kg); E_1 is the carbon emission coefficient of the truck (kg/L); D_l is the total mileage of the truck with no load (km); D_k is the total mileage of the truck with heavy load (km); t_η is the total time of the truck idling fuel consumption (h); η is the idling fuel consumption rate (L/h); t_η is the total time of the truck

idling (h); ρ_l and ρ_k are the fuel consumption rate (L/km) of the truck with no load and full load, which are determined by the speed and the load [46], as shown in Eq. (5),

$$\rho(v, l) = av^2 + bv + cl + dvl + e \quad (5)$$

where $a = 0.02$, $b = -1.67$, $c = 0.46$, $d = 0.03$, $e = 51.17$ [47].

3.2.3. Sub-objective function F_3

In this paper, the minimum carbon emission of quay cranes is identified as the third sub-objective function to measure the pollution caused by quay crane work operations in the surrounding environment of the port. Since the carbon emissions generated by the quay crane operation are positively related to power consumption, the port cost can be saved while reducing the carbon emissions from the quay crane. The sub-objective function F_3 can be calculated by the working energy consumption of the quay crane during working operations and in moving operations, which can be determined by Eq. (6),

$$F_3 = E_2 \left\{ \lambda_1 \sum_{i=1}^v [(TD_i - TS_i) \bullet TC_i + (TD_i - TV_i) \bullet \Delta VC_{it}] + \lambda_2 \sum_{i=1}^v \Delta VC_{it} \right\} \quad (6)$$

where F_3 is the third objective function (kg); E_2 is the grid reference emission factor (kg/kWh); λ_1 is the working energy consumption of the quay crane (kWh/h); λ_2 is the energy consumption of quay cranes in moving operation (kWh/time); TD_i is that vessel i finishes working operations time; TS_i is that vessel i starts working operations time; VC_i is the number of quay cranes scheduled for working operations; t is the time point of the quay cranes assisting vessel i in working operations; ΔVC_{it} is the number of quay cranes that move from the near berth at time t to assist vessel i in operations; TV_i is the start time of the adjacent quay crane carrying out an operation for the vessel i .

3.3. Determination of constraints

In light of the actual situation of the container port, the constraints of the TEU-BQCT model are determined from three aspects: the vessel berthing process, the quayside crane, and the container truck.

3.3.1. Vessel berthing process constraints

Following the vessel berthing process, the vessel berthing constraints are determined as follows:

$$TA_i = TO_i + \Delta TA_i, \forall i \in V \quad (7)$$

$$\Delta TA = f_{Erlang}(k_{TA}, \mu_{TA}) \quad (8)$$

$$TB_i \geq TA_i, \forall i \in V \quad (9)$$

$$TC_i = TB_i + TG_0, \forall i \in V \quad (10)$$

$$TS_i \geq TC_i, \forall i \in V \quad (11)$$

$$TS_i - TA_i \leq TW_i, \forall i \in V \quad (12)$$

$$TD_i - TS_i = VE_i \sqrt{(CE_n \times \sum_{t \in T} VC_{it})}, \forall i \in V \quad (13)$$

$$TE_i \geq TD_i, \forall i \in V \quad (14)$$

$$TF_i = TE_i + TG_0, \forall i \in V \quad (15)$$

$$2(u-1)W - R(1 - \mu_{iu}) \leq TB_i \leq (2u-1)W - TG_0 - R(1 - \mu_{iu}), \forall i \in V \quad (16)$$

$$2(u-1)W - R(1 - \nu_{iu}) \leq TE_i \leq (2u-1)W - TG_0 - R(1 - \nu_{iu}), \forall i \in V \quad (17)$$

$$\sum_{u \in T} \mu_{iu} = 1, \forall i \in V^L \quad (18)$$

$$\sum_{u \in T} \nu_{iu} = 1, \forall i \in V^L \quad (19)$$

$$\sum_{j=B} \sum_{k \in VO} (x_{ijk} \times BD_j) \geq VD_i, \forall i \in V \quad (20)$$

$$\sum_{j=B} \sum_{k \in VO} (x_{ijk} \times BL_j) \geq VL_i, \forall i \in V \quad (21)$$

$$\sum_{i \in V} x_{ijk} \leq 1, \forall j \in B, \forall k \in VO \quad (22)$$

$$\sum_{j=B} \sum_{k \in VO} x_{ijk} = 1, \forall i \in V \quad (23)$$

$$x_{ijk} \times TA_i \leq x_{ij(k+1)} TA_i, \forall i, i' \in V, \forall j \in B, \forall k \in VO \quad (24)$$

Constraint (7) means the calculation method of the vessel actual arrival time; Constraint (8) represents that the vessel arrival offset time should meet the Erlang distribution; Constraint (9) represents that when the vessel enters the port, the time for sailing into the channel ought to be later than the time for the vessel arriving at the port; Constraint (10) represents the calculation method of the vessel sailing out of the channel; Constraint (11) shows that the working time of the vessel ought to be later than the time for the vessel sailing out of the channel; Constraint (12) shows that the vessel waiting time should not be later than the waiting time threshold; Constraint (13) represents the calculation method of the actual loading and unloading operation time; Constraint (14) represents that when the vessel leaves the container port, the time for sailing into the channel ought to be later than the time for leaving the berth; Constraint (15) represents the calculation method for the time when the vessel leaves the container port; Constraints (16)-(19) mean that vessels are affected by tidal factors, and large vessels are only allowed to enter the container port through the waterway at the tide level; Constraints (20)-(21) mean that the berth of the vessel should meet the requirements of the vessel draught and length; Constraint (22) means that only one vessel is permitted to load and unload at each berth at a time; Constraint (23) shows that the number of berths for the vessel is only once. Constraint (24) shows that if vessels i and i' are the k -th and $(k+1)$ -th to be served, then the service time of vessel i should be earlier than that of vessel i' .

3.3.2. Quay crane constraints

By the quay crane loading and unloading process, the constraints of the quay crane operation are determined as follows:

$$\sum_{i=1}^v q_{in} = 1, \forall n \in C, \forall t \in T \quad (25)$$

$$\sum_{n=1}^c q_{in} (t - TS_i) (TD_i - t) \geq 0, \forall i \in V, \forall t \in T \quad (26)$$

$$\sum_{n=1}^v q_{in} = VC_{it}, \forall i \in V, \forall t \in T \quad (27)$$

$$VCm_i \leq \sum_{n \in C} q_{in} \leq VCM_i, \forall i \in V \quad (28)$$

$$\sum_{i=1}^v \sum_{n=1}^c q_{in} \leq c, \forall t \in T \quad (29)$$

$$\Delta VC_{it} = VC_{it} - VC_{it-1}, \forall i \in V, \forall t \in T \quad (30)$$

$$q_{i(n-1)} + q_{i(n+1)} - q_{in} = \begin{cases} -1 & , \forall i \in V, n \in C, \forall t \in T \\ 0 & , \forall i \in V, n \in C, \forall t \in T \\ 1 & \end{cases} \quad (31)$$

Constraint (25) means that each quayside crane can only serve one vessel at the same time; Constraint (26) indicates that the quay crane operations time on the vessel should be within the loading and unloading period of that vessel. Constraint (27) represents that the number of quayside cranes serving vessel i is equal to allocating to vessel

i ; Constraints (28) means that the upper and lower limits of the quay crane allocation meet the requirements of vessel working restrictions; Constraint (29) shows that the number of quayside cranes under working operations in container ports is less than the total number of quayside cranes in container ports; Eq. (30) defines a method of calculating the number of quay cranes for mobile auxiliary operations; Constraint (31) means that the quay crane is not permitted to step over other quay cranes.

3.3.3. Container truck constraints

Following the situation of the truck collection operation, the constraints of the truck collection operation are determined as follows:

$$\sum_{n=1}^c CK_{nt} \leq M \quad (32)$$

$$TH_{ij} = D_{ij} / v_h, \forall i \in V, \forall j \in B \quad (33)$$

$$TL_{ij} = D_{ij} / v_l, \forall i \in V, \forall j \in B \quad (34)$$

$$v_h \sim N(v_h; \mu_{vh}, \delta_{vh}^2) \quad (1)$$

$$v_l \sim N(v_l; \mu_{vl}, \delta_{vl}^2) \quad (2)$$

$$CE_n = CK_{nt} / \max(TH_{ij} + TL_{ij} + 1/CF_0, CK_{nt}/CE_0), \forall n \in C, \forall t \in T \quad (37)$$

Constraint (32) means that the number of working trucks at time t should not surpass the total number of available trucks in the container port; Constraints (33)-(34) represent the empty container and heavy-load transportation time when vessel i is docked at berth j ; Constraints (35)-(36) mean that the no-load and heavy-load speeds of the truck follow a normal distribution; Eq. (37) defines the calculation method of actual working efficiency of quay crane.

3.3.4. Other constraints

$$x_{ijk} \in \{0, 1\}, \forall i \in V \quad (38)$$

$$q_{in} \in \{0, 1\}, \forall i \in V, \forall n \in C \quad (39)$$

$$\mu_{iu} \in \{0, 1\}, \forall i \in V \quad (40)$$

$$\nu_{iu} \in \{0, 1\}, \forall i \in V \quad (40)$$

Eq. (38)-(41) define 0–1 variables.

3.4. Determination of dependent variables

Based on the above constraints, the relationship between the dependent variable and the input variable is determined, and the objective function value can be calculated. The specific process is determined as follows:

Step 1 Data initialization. Let $i = 1$, go to Step 2;

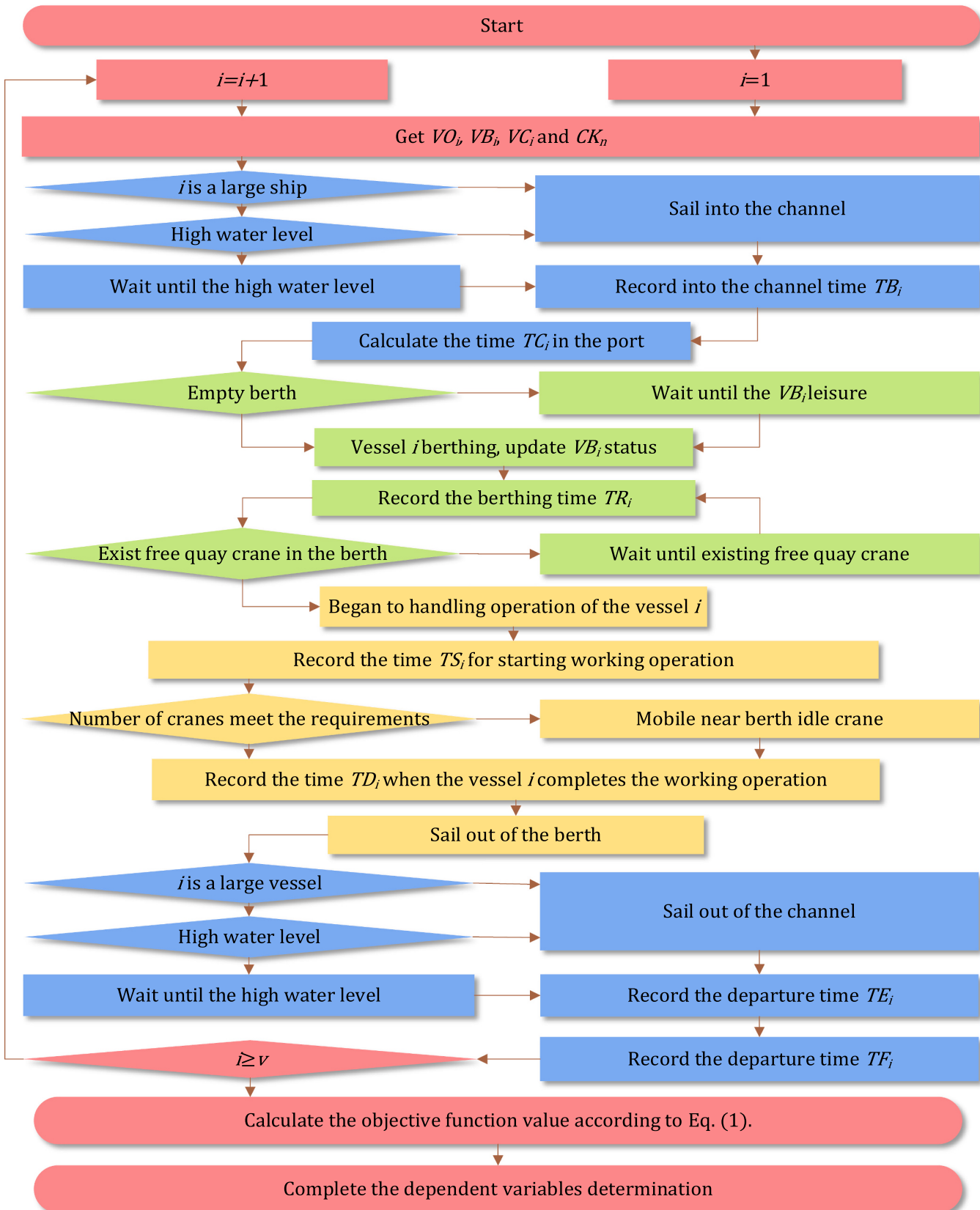
Step 2 Retrieve data. According to the berthing sequence VO_i , obtain the berthing berth VB_i of the vessel whose berthing sequence is i , the number of allocated quayside cranes VC_i , and the number of allocated trucks CK_n , and then go to Step 3;

Step 3 Determine the type of vessel. If vessel i is large, go to Step 4, otherwise, skip to Step 6;

Step 4 Determine the water level at this time. If the water level is high, skip to Step 6, if not, go to Step 5;

Step 5 Compute the time for the vessel sailing into the channel when the water level rises. Vessel i waits at the anchorage outside the port until the water level is high, then vessel i starts to enter the channel. Calculate the start time TB_i for the vessel i sailing into the channel, and skip to Step 7;

Step 6 Compute the time when the vessel sails into the channel. Vessel i starts to enter the channel. Calculate the start time TB_i for the

**Fig. 1.** Determination of dependent variables flowchart.

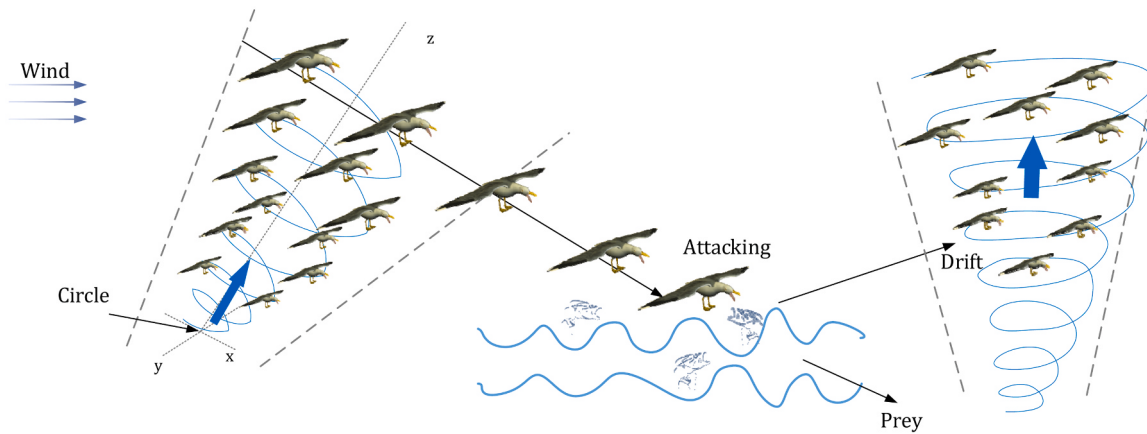


Fig. 2. Migration and predation behavior of seagulls.

vessel i sailing into the channel, and go to Step7;

Step 7Calculate the time for the vessel sailing out of the channel. Calculate and record the time TC_i of vessel i entering the port according to Eq. (10), and go to Step 8;

Step 8Determine the vacancy of the berth. If the berth VB_i is idle, go to Step9; if not, skip to Step10;

Step 9Calculate the time when the vessel starts working operations. When vessel i berths, update the usage status of berth VB_i , record the berthing time TS_i of berthing vessel i , and go to Step11;

Step 10Calculate the time required for anchorage to wait for the vessel to start loading and unloading operations. Vessel i waits at anchorage in the port until berth VB_i is free, and then berths. Update the usage status of berth VB_i , record the berthing time TS_i of vessel i , and transfer to Step11;

Step 11Determine whether the quay crane meets the predetermined requirements. If the number of continuous free quayside cranes at the berth VB_i of vessel i and its adjacent berths meet the requirements of VC_i , go to Step 12, else skip to Step 13;

Step 12Compute the time when the vessel finishes working operations when the quayside cranes meet the predetermined requirements. Compute the quay crane's actual working efficiency CE_n according to the Eq. (37). Calculate and record the vessel working service completion time TD_i following the Eq. (13), update the berth and quay crane idle time, and skip to Step 14;

Step 13Compute the time for the vessel to end working operations when the quayside cranes do not meet the predetermined requirements. Compute the actual working efficiency CE_n according to the Eq. (37). Record the number of quayside cranes that can be loaded and unloaded at this time as VC_{it} . After the adjacent quay cranes are idle, under the condition that the continuity constraints of the quay cranes are satisfied, calculate and record the service completion time TD_i of vessel loading and unloading operations according to the Eq. (13), and update berth and quay crane idle time, go to Step 14;

Step 14Determine the type of vessel. If vessel i is a large vessel, go to Step 15, otherwise, go to Step 17;

Step 15Determine the water level at this time. If the water level is high, go to Step17, otherwise, go to Step16;

Step 16Calculate the time to wait for the vessel to enter the channel when the water level rises. Vessel i is at the anchorage in the port and waits until the water level is at a high water level, and then, starts to sail into the channel. Record the start time TE_i sailing out of the channel, and skip to Step 18;

Step 17Compute the time when the vessel sails into the channel. Vessel i starts to sail into the channel. Record the start time TE_i for vessel i sailing into the channel, and transfer to Step 18;

Step18Compute the departure time of the vessel. Vessel i sails out of the port. Calculate and record the departure time TF_i according to the

Eq. (15), and go to Step 19;

Step 19Judge whether the calculation of all arriving vessels is completed. If $i \geq v$, go to Step21, otherwise, go to Step20;

Step 20Do the next vessel calculation. Let $i = i + 1$, redirect to Step2;

Step 21Calculate the objective function value according to Eq. (1).

Step 22Complete the determination of all dependent variables.

The flow chart of determining dependent variables is shown in Fig. 1:

4. Chaos quantum adaptive seagull optimization algorithm (CQASOA) and TEU-BQCT model solving method

Aiming at the solution problem of the container port dispatching scale model, given the good performance of SOA in other similar fields [48,49], this paper attempts to adopt SOA to solve the TEU-BQCT model.

4.1. Standard Seagull optimization algorithm (SOA)

SOA is divided into migration behavior and attack behavior[3]. These two behaviors can be depicted by Fig. 2. A brief description of the algorithm process is as follows:

4.1.1. Migratory behavior

(1) **Avoid collision:** The formula for updating the new position of the seagull is shown Eq. (42). Variable s determined as shown in Eq. (43),

$$C'_s = A \times P_s^t \quad (42)$$

where C'_s means a new location that does not make a collision with adjacent seagulls; t means the current number of iterations; P_s^t means the current position of the seagulls.

$$A = f_c - [t \times (f_c / T_{\max})] \quad (43)$$

The value of variable A varies linearly with f_c , take $f_c = 2$. T_{\max} is the maximum number of iterations.

(2) **Best position direction:** To avoid collision between seagulls, the seagulls will move towards the best seagull location direction as Eq. (44),

$$M_s^t = B \times (P_{bs}^t - P_s^t) \quad (44)$$

where M_s^t represents the best seagull position direction; P_{bs}^t is the best seagull position; B is a random number, and its expression is determined as Eq. (45),

$$B = 2 \times A^2 \times r_d \quad (45)$$

Table 2
Cat chaotic map and random point distribution comparison table.

Interval	Random	Cat Map
[0, 0.1)	5188	5049
[0.1, 0.2)	4995	4920
[0.2, 0.3)	5039	4975
[0.3, 0.4)	5068	5028
[0.4, 0.5)	4879	4981
[0.5, 0.6)	4867	5048
[0.6, 0.7)	5116	5058
[0.7, 0.8)	4860	4962
[0.8, 0.9)	5023	4999
[0.9, 1)	4965	4980
Variance	10,865.4	1808.4

where r_d is a random number between [0,1].

(3) Approaching the optimal seagull position: After the individual seagull reaches a location that does not conflict with other seagulls, the seagull will update its position to make it closer to the optimal seagull position, as Eq. (46),

$$D_s^t = |C_s^t + M_s^t| \quad (46)$$

where D_s^t is a new location for seagulls to migrate.

4.1.2. Aggressive behavior

When seagulls attack their prey, they need fly downward in a spiral, and continuously alter the direction and angle of the attack, which can be expressed as Eq. (47),

$$\begin{cases} X = r \times \cos\theta \\ Y = r \times \sin\theta \\ Z = r \times \theta \\ r = u \times e^{\theta v} \end{cases} \quad (47)$$

where r is the radius of the spiral flight when the seagull is attacking; θ is a random angle value in the interval $[0, 2\pi]$; u and v are constants; e is the base of the natural logarithm.

The seagull attack in a spiral can be expressed as Eq. (48),

$$P_s^t = D_s^t \bullet X \bullet Y \bullet Z - P_{bs}^t \quad (48)$$

where P_s^t means the attack location of the seagull in the spiral motion.

The SOA iteration formula can be obtained by the synthesis of Eqs. (42) to (48),

$$P_s^{t+1} = P_{bs}^t + |B \bullet P_{bs}^t + (A - B)P_s^t| \bullet X \bullet Y \bullet Z \quad (49)$$

4.1.3. SOA existing problems and improvement methods

Although SOA has the advantages of better optimization performance and faster calculation speed than traditional optimization algorithms, it still has the problem of weak global perturbation ability and easily falling into the local optimal solution. Therefore, based on the chaotic map, the population initialization method is improved to increase the global distribution of the SOA initial population; Based on the quantum revolving gate and the quantum NOT gate, the population iterative update process is made better to enhance the calculation speed; The nonlinear convergence factor is introduced to increase the global disturbance capability in the early stage and the local search capability in the later stage. Then, a novel chaotic quantum adaptive seagull optimization algorithm is proposed, named CQASOA.

4.2. Design of chaos quantum adaptive seagull optimization algorithm (CQASOA)

4.2.1. Design of chaos seagull optimization algorithm (CSOA)
Compared with random algorithms, chaotic maps are more ergodic. In this paper, based on the chaotic map, the initialization process of the

SOA population is improved, so that the generated initial population has better diversity. The chaotic maps commonly used in optimization algorithms are Logistic mapping [50], Tent mapping [51], An mapping [52], and so on. Compared with other chaotic mappings, Cat mapping has better distribution characteristics [17], so the initialization form of the Cat chaotic map sequence is proposed in the paper. The Cat mapping expression can be as Eq. (50),

$$\begin{cases} x_{n+1} = (x_n + y_n) \bmod 1 \\ y_{n+1} = (x_n + 2y_n) \bmod 1 \end{cases} \quad (50)$$

where $x \bmod 1 = x - [x]$ means that only the fractional part of x is taken; x_n, y_n are the values of the cat mapping parameter calculated for the n -th time.

The two-dimensional Cat mapping matrix form expression is as Eq. (51),

$$\begin{bmatrix} x_{n+1} \\ y_{n+1} \end{bmatrix} = \begin{bmatrix} 1 & 1 \\ 1 & 2 \end{bmatrix} \begin{bmatrix} x_n \\ y_n \end{bmatrix} \bmod 1 = C \begin{bmatrix} x_n \\ y_n \end{bmatrix} \bmod 1 \quad (51)$$

$$\text{where } C = \begin{bmatrix} 1 & 1 \\ 1 & 2 \end{bmatrix} \text{ and } |C| = 1.$$

The Cat map and random point-point distribution were tested 50,000 times, and their distribution in the 0–1 interval was calculated as shown in Table 2. By calculating the variance of the interval distribution case, it can be seen that the Cat map has a better distribution over the entire solution space.

In the process of population initialization, if the number of population samples is n , then the entire initialized population can be expressed as follows $\mathbf{x} = [x_1, x_2, \dots, x_n]$. The population individuals x_1 and auxiliary parameter y_1 are randomly generated within the population definition domain, x_2 and y_2 are calculated according to Eqs. (50) and (51), and the other populations are calculated sequentially. The calculated \mathbf{x} is the population.

4.2.2. Design of quantum seagull optimization algorithm (QSOA)

Quantum computing is an emerging computing model based on quantum mechanics. Given the superposition principle of quantum mechanics, computing efficiency is improved. In quantum computing, the logical transformation function of qubits is usually realized through a series of unitary transformations. A quantum device that implements logical transformations within a certain time interval is called a quantum gate. Commonly used single-bit quantum gates include the phase gate, $\pi/8$ gate, Hadamard gate, quantum revolving gate, and so on. A quantum revolving gate can be represented as Eq. (52),

$$|\varphi'\rangle = R|\varphi\rangle = \begin{bmatrix} \cos\Delta\varphi & -\sin\Delta\varphi \\ \sin\Delta\varphi & \cos\Delta\varphi \end{bmatrix} \begin{bmatrix} \cos\varphi \\ \sin\varphi \end{bmatrix} = \begin{bmatrix} \cos(\varphi + \Delta\varphi) \\ \sin(\varphi + \Delta\varphi) \end{bmatrix} \quad (52)$$

where $|\varphi\rangle$ is the phase before the quantum revolving door transformation; $|\varphi'\rangle$ is the phase after the quantum revolving door transformation; $\Delta\varphi$ is the phase rotation radian of the quantum revolving door.

Due to the high efficiency of quantum computing, the computational performance and convergence speed of intelligent optimization algorithms can be improved through quantum revolving gates [53]. The quantum revolving gate is tried to enhance the convergence speed and precision of SOA by combining Eqs. (52) and (49), and the following expression (Eqs. (53) to (55)) will be satisfied:

$$\varphi = P_{bs}^t \quad (53)$$

$$\varphi' = P_s^{t+1} \quad (54)$$

$$\Delta\varphi = |B \bullet P_{bs}^t + (A - B)P_s^t| \bullet X \bullet Y \bullet Z \quad (55)$$

The direction of the corner $\Delta\varphi$ can be selected according to the following rules: When $R \neq 0$, the direction is $-\text{sgn}(R)$; When $R = 0$, the

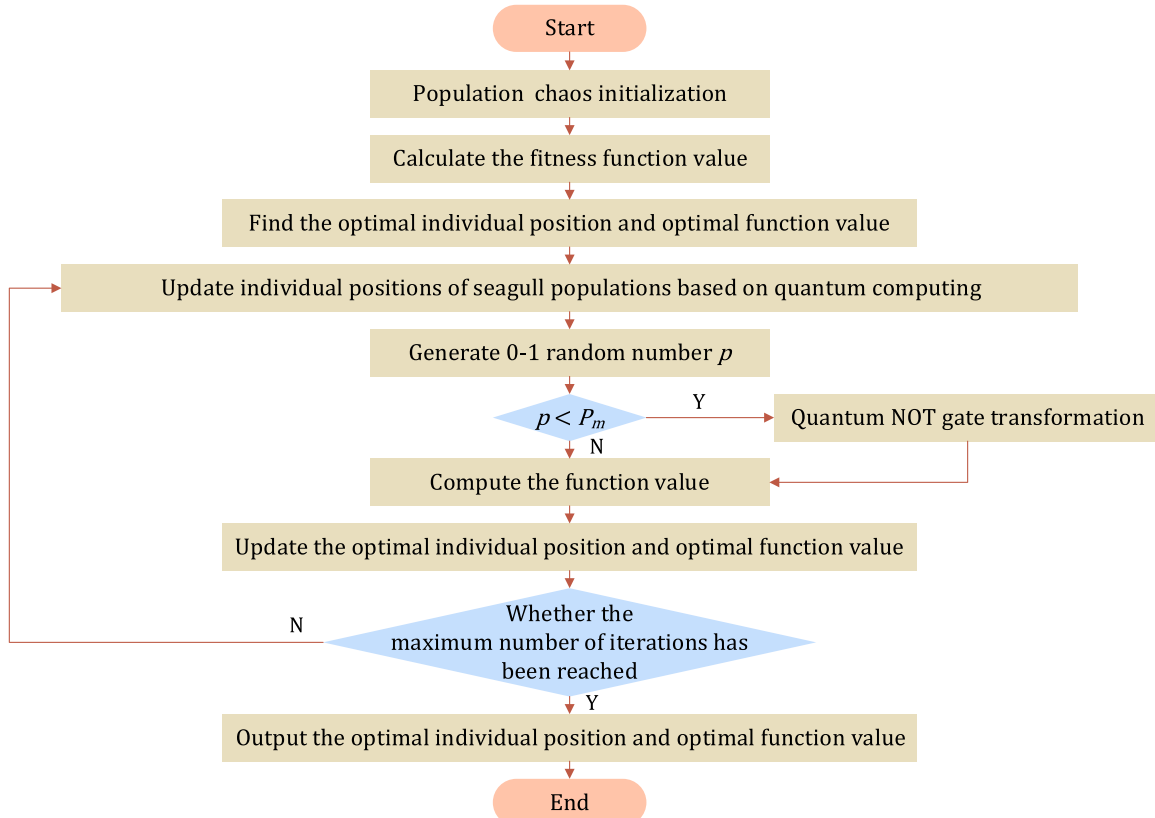


Fig. 3. CQASOA flowchart.

direction can be positive or negative.

In quantum computing, quantum phase transitions can be achieved through quantum NOT gates. In the intelligent optimization algorithm, the global traversal range of the algorithm can be increased according to the performance of the quantum NOT gate [54]. For the problem of falling into the local optimal solution easily, this paper attempts to globally perturb the individual location of the population via the quantum NOT gate to escape from the local optimum and enhance the global search ability of SOA. The quantum NOT gate expression can be determined as Eq. (56),

$$\begin{bmatrix} 0 & 1 \\ 1 & 0 \end{bmatrix} \begin{bmatrix} \cos\varphi \\ \sin\varphi \end{bmatrix} = \begin{bmatrix} \sin\varphi \\ \cos\varphi \end{bmatrix} = \begin{bmatrix} \cos(\pi/2 - \varphi) \\ \sin(\pi/2 - \varphi) \end{bmatrix} \quad (56)$$

where φ is the transformation phase of the quantum NOT gate, which can be determined by Eq. (53).

In QSOA, the probability of the quantum phase passing through the quantum NOT gate is set to p_m . After passing through the quantum revolving gate, a random number p is generated between $[0,1]$. If $p < p_m$, it passes through the quantum NOT gate, otherwise it enters the next iterative process.

4.2.3. Design of adaptive parametric seagull optimization algorithm (ASOA)

Considering that the SOA has the problems of weak disturbance ability in the early stage and insufficient local exploration ability in the later stage, adaptive parameters are introduced. In SOA, the values of parameters A and B affect the global perturbation ability and local exploration capability. And parameter A is related to B . Therefore, this paper attempts to improve the linear convergence parameter A . A nonlinear function is considered added to establish a functional relationship between the number of iterations t and the convergence parameter A , to strengthen the early global disturbance capability and later local development capability. The specific expression is as Eq. (57),

Table 3
Coding Rule Matrix Numerical Example of individual p .

Vessel ID		1	2	3	4	5	6
First row: Berthing sequence VO	SEAGULL [p, 1,:]	3	5	4	2	1	6
Second row: Berthing position VB	SEAGULL [p, 2,:]	3	1	2	4	3	4
Third row: Quantity of allocated VC	SEAGULL [p, 3,:]	2	3	2	1	5	5
Fourth row: Quantity of allocated VK	SEAGULL [p, 4,:]	11	8	14	9	10	13

$$A = f_c \{ \cos[\pi \bullet (t/t_{\max}) + 1] \}/2 \quad (57)$$

where variable A changes nonlinearly and adaptively with f_c , take $f_c = 2$, following the addition of the number of iterations, the variable A declines nonlinearly from 2 to 0; t is the current number of iterations; T_{\max} is the maximum number of iterations.

4.2.4. Design of chaos quantum adaptive seagull optimization algorithm (CQASOA)

Because the three algorithms CSOA, QSOA, and ASOA have their advantages, this paper attempts to integrate the above three improved methods to obtain CQASOA. The flowchart of CQASOA are shown in Fig. 3:

4.3. The design of the solution method for solving the TEU-BQCT model based on CQASOA

4.3.1. Formulation of coding rules for TEU-BQCT model

Aiming at facilitating the expression of optimization variables in the process of model solving, a natural number encoding matrix of berthing

order, assigned berth, assigned quay crane number, and assigned container truck number is constructed. The number of matrix columns is v , which depends on the total number of vessels sailing into the port; The number of rows in the matrix is four, the first row represents the order of vessels sailing into the port (**VO**), the second row means the serial number of the berth to be parked (**VB**), the third row represents the serial number of allocated quay cranes (**VC**), and the fourth row is the number of sets of trucks (**VK**). A simple numeric instance of the coding method is shown in Table 3. The first column of the coding matrix is taken as an example: the vessel is numbered 1, the order of vessels sailing into the port is 3, the serial number of the berth to be parked is 3, the number of allocated quay cranes is 2, and the number of allocated trucks is 11.

4.3.2. Design of feasible-integration algorithm (F-IA) for TEU-BQCT model

According to the port operation process, VO_i , VB_i , VC_i , and VK_i are natural numbers, so the coding matrix is defined as a matrix of natural numbers. The iterative calculation result of CQASOA is a real number, thus, a feasible-integration algorithm (F-IA) suitable for the TEU-BQCT model is designed to make the optimization variables of each update iteration meet the requirements of natural numbers.

The algorithm is mainly divided into four parts, which respectively perform feasible integer processing for the four-row vectors of the encoding matrix. In this paper, the coding matrix is **SEAGULL** [$p, :, :$] individual p as an example (where **SEAGULL** [$p, 1, q$] represents the value corresponding to the q -th column of the first row; **seagull_size** is the population size), and the design process is introduced as follows:

Step1Let $p = 1$, go to Step2;

Step2If the variables in the first row **SEAGULL** [$p, 1, :$] are not equal, then go to Step3, otherwise go to Step4;

Step3Sort **SEAGULL** [$p, 1, :$] by numerical size, and use the corresponding numerical order as the vessel berthing order **SEAGULL₁** [$p, 1, :$], let **SEAGULL_NEW** [$p, 1, :$] = **SEAGULL₁** [$p, 1, :$], go to Step5..

Step4Sort **SEAGULL** [$p, 1, :$] by numerical size, and use the corresponding numerical order as the vessel berthing order **SEAGULL₁** [$p, 1, :$], where for vessels with equal values, the order is determined according to the berthing order before evolution, let **SEAGULL_NEW** [$p, 1, :$] = **SEAGULL₁** [$p, 1, :$], go to Step5..

Step5Let $q = 1$, go to Step6;

Step6Round up the berth **SEAGULL** [$p, 2, q$] of the q -th vessel in individual p to obtain **SEAGULL₁** [$p, 2, q$], and judge whether **SEAGULL₁** [$p, 2, q$] satisfies the berthing constraints, if so, let **SEAGULL_NEW** [$p, 2, q$] = **SEAGULL₁** [$p, 2, q$], if not the natural number **SEAGULL₂** [$p, 2, q$] is randomly generated under the condition of satisfying the berthing constraint, and **SEAGULL_NEW** [$p, 2, q$] = **SEAGULL₂** [$p, 2, q$], go to Step7..

Step7If $q \geq v$, go to Step9, otherwise go to Step8..

Step8Let $q = q + 1$, go to Step6..

Step9Let $q = 1$, go to Step10..

Step10Round off the number **SEAGULL** [$p, 3, q$] of the serial number of allocated quayside cranes to the q -th vessel in individual p to obtain **SEAGULL₁** [$p, 3, q$], and judge whether **SEAGULL₁** [$p, 3, q$] satisfies the constraints related to quay cranes, if so, let **SEAGULL_NEW** [$p, 3, q$] = **SEAGULL₁** [$p, 3, q$], else under the condition that the constraints are met, the natural number **SEAGULL₂** [$p, 3, q$] is randomly generated, and **SEAGULL_NEW** [$p, 3, q$] = **SEAGULL₂** [$p, 3, q$], go to Step11..

Step11If $q \geq v$, go to Step13, otherwise go to Step12..

Step12Let $q = q + 1$, go to Step10..

Step13Let $q = 1$, go to Step14..

Step14Round the number **SEAGULL** [$p, 4, q$] for the number of trucks allocated to the q -th vessel in individual p to get **SEAGULL₁** [$p, 4, q$], and judge whether **SEAGULL₁** [$p, 4, q$] satisfies the truck constraints, if so, let **SEAGULL_NEW** [$p, 4, q$] = **SEAGULL₁** [$p, 4, q$], else under the condition that the constraints are met, randomly generate the natural number **seagull₂** [$p, 4, q$], let **SEAGULL_NEW** [$p, 4, q$] = **SEAGULL₂** [$p, 4, q$], enter Step15..

Step15If $q \geq v$, go to Step17, else go to Step16..

Step16Let $q = q + 1$, go to Step14..

Step17If $p \geq seagull_size$, go to Step19, otherwise go to Step18..

Step18Let $p = p + 1$, go to Step2..

Step 19Complete feasible integration.

In F-IA, Steps 2 to 4 are feasible-integer processing for vessel berthing sequence; Steps 5 to 8 are feasible-integer processing for berthing berths; Steps 9 to 12 are feasible-integer processing for allocating the number of quay cranes; Steps 13 to 16 are the feasible-integer processing for allocating trucks.

4.3.3. Construction of external penalty function adapted to TEU-BQCT model

Aiming at the vessel docking time constraint (12) and the number of truck operations (32), the external penalty method is tried used as solving the TEU-BQCT [55]. Based on the model objective function construction method of Eq. (1), the external penalty function auxiliary function **F_punish** is constructed as Eq. (58),

$$F_punish = \omega_1 \cdot k_1 \cdot F_punish_1 + \omega_2 \cdot k_2 \cdot F_punish_2 + \omega_3 \cdot k_3 \cdot F_punish_3 \quad (58)$$

where **F_punish** is the auxiliary function of the objective function **F**; **F_punish₁**, **F_punish₂**, and **F_punish₃** are the auxiliary functions of the sub-objective functions **F₁**, **F₂**, and **F₃**; ω_1 , ω_2 , and ω_3 are the weight adjustment factors; k_1 , k_2 , and k_3 are the quantities level balance factor. (The weight adjustment factor and the magnitude balance coefficient both satisfy the condition of Eq. (2)).

The auxiliary functions **F_punish₁**, **F_punish₂**, and **F_punish₃** can be determined as Eqs. (59) to (61),

$$F_punish_1 = F_1 + \mu_1 \sum_{i=1}^v \max[(TS_i - TA_i) - TW_0, 0] \quad (59)$$

$$F_punish_2 = F_2 + \mu_2 \sum_t^T [\sum_{n=1}^c \max(CK_{nt} - M, 0)] \quad (60)$$

$$F_punish_3 = F_3 \quad (61)$$

where **F₁**, **F₂**, and **F₃** are the sub-objective function values 1–3, which are determined by Eqs. (3), (4), and (6); **TS_i** is the time when vessel i starts working operations; **TA_i** is the actual arrival time of vessel i ; **TW₀** is the vessel's maximum allowable waiting time; **CK_{nt}** is the number of trucks serving quayside crane n at time t ; **M** is the total number of trucks that can be served by container ports; μ_1 and μ_2 are penalty factors, subject to Eqs. (62) and (63),

$$\mu_1 = \exp(T_{\max}) \quad (62)$$

$$\mu_2 = \exp(T_{\max}) \quad (63)$$

During the CQASOA update iteration, the auxiliary function is replaced by the objective function for function value calculation. If the requirements of constraints (12) and (32) cannot be met, and the result approaches $+\infty$, the result will be eliminated in the iterative process. And then a solution meeting the constraints will be obtained.

4.3.4. Process design of solving TEU-BQCT model based on CQASOA

CQASOA was proposed to solve the TEU-BQCT model, in order to optimize the scheduling scheme to obtain a vessel berthing sequence - berthing number - service quay cranes number - service trucks number scheduling scheme with the shortest berthing time and the lowest carbon emission of the vessels. The process of solving the TEU-BQCT model is designed as follows:

Step1Let $t = 1$, go to Step2;

Step2Set the population size **seagull_size** and the number of iterations **T_{max}**.

Step3Following the TEU-BQCT coding rules, the chaotic population is initialized according to the Eqs. (50) and (51).

Step4Feasible-integration of the initialized population based on F-

Table 4

Basic information on large-scale port arrival vessels.

ID	VL_i	VD_i	VE_i	VCm_i	VCM_i	D_{i1}	D_{i2}	D_{i3}	D_{i4}
1	100	5	100	1	3	1831	2290	2574	3031
2	200	8	250	1	3	2499	1934	2139	2566
3	200	8	250	1	3	2499	1934	2139	2566
4	250	15	500	1	4	3114	2535	2054	2922
5	400	30	1000	1	5	3157	2861	2273	2015
6	400	30	1000	1	5	3157	2861	2273	2015

Table 5

Basic information on small-scale port arrival vessels.

ID	VL_i	VD_i	VE_i	VCm_i	VCM_i	D_{i1}	D_{i2}
1	100	5	100	1	3	1831	2290
2	200	8	250	1	3	2499	1934
3	200	8	250	1	3	2499	1934
4	250	15	500	1	4	3114	2535
5	400	30	1000	1	5	3157	2861
6	400	30	1000	1	5	3157	2861

IA;

Step5Compute the value of the auxiliary function F_punish of population;.

Step6Seek the global optimal solution and the optimal solution location;.

Step7Complete population iterative evolution based on Eqs. (49) and (52);.

Step8Randomly generate a 0–1 random number p , if $p < p_m$, go to Step9, otherwise go to Step10;.

Step9Enter the quantum NOT gate, perform quantum NOT gate transformation based on Eq. (56), and enter Step10;.

Step10If $t \leq T_{\max}$, go to Step11, otherwise go to Step12;.

Step11Let $t = t + 1$, go to Step4;.

Step 12Complete all iterative calculations and output the optimal result.

4.4. Rolling optimization mechanism

Considering the problems of vessel renewal and equipment rescheduling in ports, a rolling optimization mechanism is designed to provide a practical application scheme of the TEU-BQCT_CQASOA solution method for port managers in light of the characteristics of continuous working operations in ports. Based on the principle of "batches and times", this mechanism will process vessels in batches according to the estimated arrival time of vessels. When a batch of vessels sails into the port, if there are no vessels in the container port carrying out working operations, it will directly enter the optimization sequence, apply TEU-BQCT_CQASOA to solve the scheduling scheme, and start the optimization process; If other batches of vessels are loading and unloading, the vessels go to next batch and wait for the optimization of the previous batch of vessels to start optimization.

5. Numerical experiments

5.1. Experimental settings

In this paper, two ports in South China are taken as examples to conduct numerical experiments. Large-scale ports have 4 berths, No.1–3 berths are 400 m in length and a draft of 20 m, No.4 berth length is 400 m and the draft is 30 m, and the total number of quay cranes is 12; Small-scale ports have 2 berths and No.1 berth has a length of 400 m, the draft is 20 m, the length of No.2 berth is 400 m, the draft is 30 m, and the total number of quay cranes is 6. The water level time window in the two ports is 6 h long. The deviation time for the arrival of vessels at the port obeys the Erlang distribution, and the parameters are set as $k_{TA} = 6$

Table 6

Example value of weight adjustment factor and corresponding application.

	ω_1	ω_2	ω_3
Situation I: Concentrate on cutting down the vessel time in port	0.5	0.25	0.25
Situation II: Concentrate on cutting down truck carbon emissions	0.25	0.5	0.25
Situation III: Concentrate on cutting down the carbon emissions of quay cranes	0.25	0.25	0.5

Table 7

Calculation results of three groups of representative working conditions.

	Time of vessels in port F_1	Truck carbon emissions F_2	Quay crane carbon emissions F_3
Situation I	10.82975589	15385.84584	18185.71205
Situation II	11.44170212	14555.17091	18219.32922
Situation III	12.46912124	14989.03284	15826.06306

and $\mu_{TA} = 0.03$.

The theoretical loading and unloading efficiency of quay cranes is 2TEU/(unit·min). The upper limit for small, medium and large vessels to allow quay cranes to carry out working operations is 3, 4, and 5. The port is located in South China, the power grid benchmark emission factor is 0.8959, the grid work energy consumption of the quayside crane working operation is 120kWh/h and the mobile quay crane consumes 12kWh/time of electricity.

The no-load speed of the truck $v_h \sim N(v_h; 35, 4)$, the unit is km/h, the truck heavy-load speed $v_l \sim N(v_l; 25, 4)$, the unit is km/h. The self-weight of the truck is 4.5 tons, the idling fuel consumption rate is 2.14 L/h, the total number of trucks in the container port is 45, and the carbon emission coefficient of trucks is 2.65 kg/L. The container specification is a 20-foot container, with a gross weight of 17.5 tons and a self-weight of 2.3 tons.

In this paper, 6 vessels arriving at the port are used as a group for simulation. The upper limit for vessel waiting time is set to 24 h. **Table 4** and **Table 5** show that the vessel length (VL_i), the vessel draft (VD_i), the deadweight (VE_i), the preferred berth (VP_i), the lower limit of quay cranes serving vessels (VCm_i), the upper limit of quay cranes serving vessels (VCM_i), and the distance between the vessel i docked at berth j and the target yard (D_{ij}):

A dynamic database is completed given MySQL and the algorithm is programmed with python3.9 language. The operating environment is 7th Gen Intel(R) Core(TM) i7-7500 U, 1.99 GHz, 8.00 GB memory laptop, operating system: Windows11.

5.2. Analysis of TEU-BQCT model performance

5.2.1. Model performance analysis under different demands

For meeting the scheduling requirements of ports in different periods, the weight adjustment factors ω_1 , ω_2 , and ω_3 are introduced into the TEU-BQCT model to realize the development of matching scheduling schemes for ports with different needs. Three groups of representative

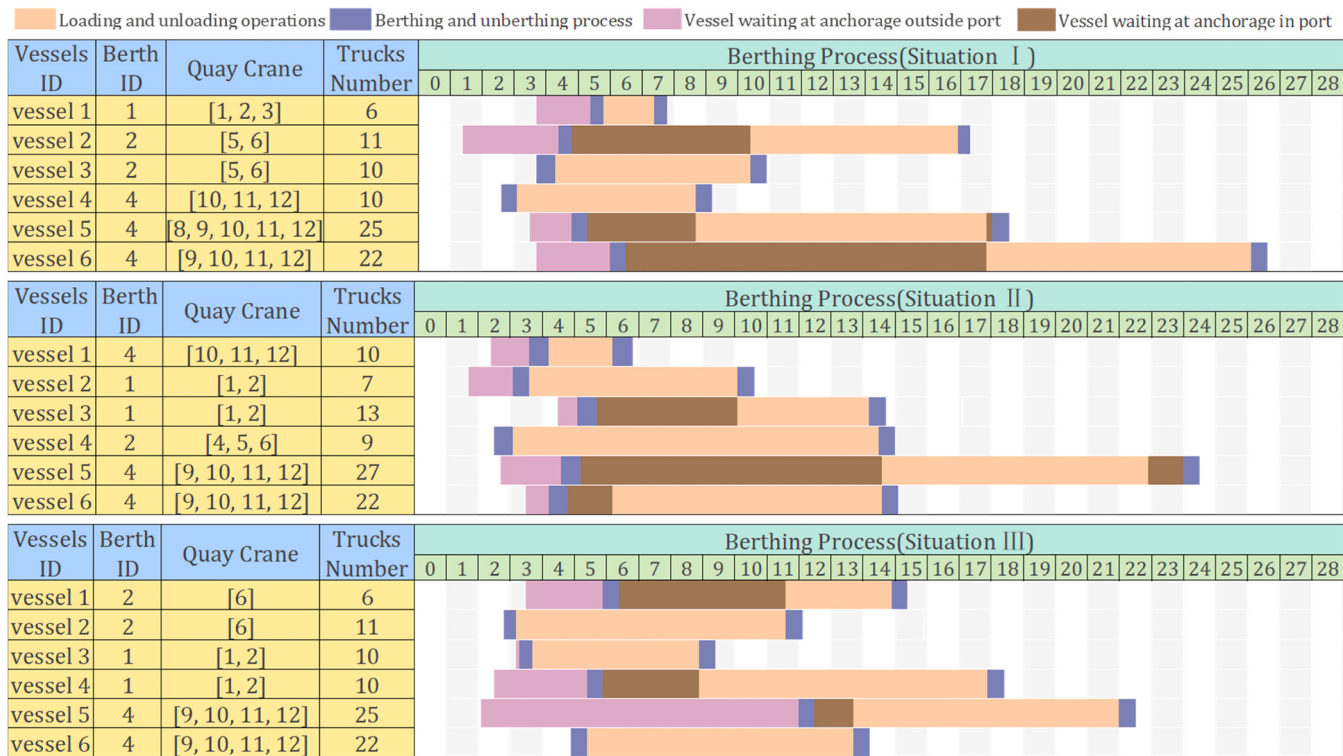


Fig. 4. Scheduling Allocation Schemes with Different Weight Coefficients.

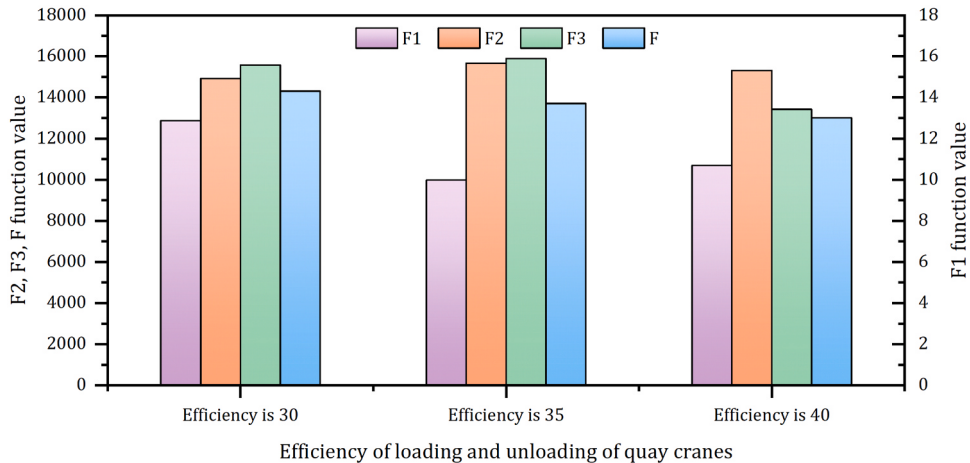


Fig. 5. Effect of the working efficiency of quay cranes.

weight values and application situations are set for examining the effect of the weight adjustment factor on the TEU-BQCT model in this paper, as shown in Table 6:

Table 6 shows the weight coefficient values in different situations:

Situation I:

When the container port is in the peak season and the number of vessels sailing into the port is large, which causes vessel congestion. It is necessary to cut down the time for vessels staying in the port and heighten the working operations efficiency of the container port. At this time, the value of the weight ω_1 should be increased.

Situation II:

The fuel emission of trucks will reduce the environmental quality. To prevent the generation of haze, considering the environmental sensitivity, the value of the weight ω_2 should be increased.

Situation III:

The quay crane operation will consume electric energy. If the power consumption of the port quay crane is too high, it will lead to increasing port carbon emissions. Considering the reduction of the work energy consumption generated by the quay crane operation, the value of the weight ω_3 should be increased.

The simulation calculation is carried out according to the above three sets of weight coefficient values. Under the same conditions, the calculation results are exhibited in Table 7, and the scheduling scheme is shown in Fig. 4:

By comparing Situation II and III and Situation I, it is found that aiming at reducing the vessel turnaround time, the value of weight coefficient ω_1 can be increased, so that the vessels turnaround time of Situation I can be reduced by 5.35% and 13.15% respectively; In comparison with Situation I and III, the truck carbon emissions of Situation II are decreased by 5.40% and 2.58%, which reveals that a dispatch plan

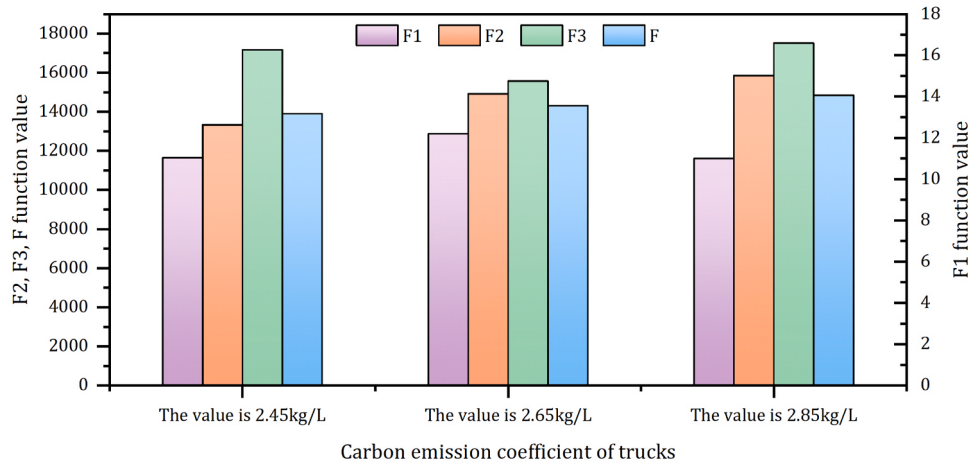


Fig. 6. Effect of the carbon emission coefficient of trucks.

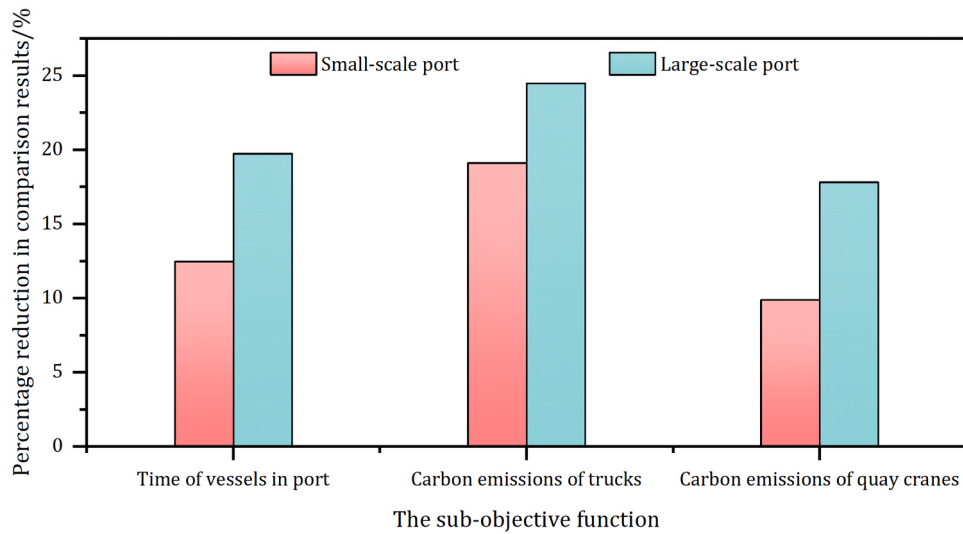


Fig. 7. Effect of the port size.

can be generated for reducing the carbon emissions of the collectors by increasing the value of the weight coefficient ω_2 ; Following increasing the weight coefficient ω_3 , the carbon emissions of *Situation III* quay cranes are reduced by 12.98% and 13.14% respectively, indicating that the weight coefficient ω_3 can be used to generate a dispatch plan to lower the carbon emissions of quay cranes.

The above test shows that the TEU-BQCT model can achieve the expected goal of meeting the different needs of the port in different periods, indicating that the attempt to introduce the weight coefficient is feasible.

5.2.2. Robustness analysis of the model performance

1) Effect of the working efficiency of quay cranes.

First, to test the effect of changes in the quay crane handling efficiency on the TEU-BQCT model, we set three different quay crane handling efficiencies, 30TEU/h, 35TEU/h, and 40TEU/h. The test results are shown in Fig. 5. Compared with the case where the loading and unloading efficiency is 30TEU/h, the objective function F of the other two cases decreases by 4.38% and 9.99%.

In Fig. 5, following the increase in loading and unloading efficiency, each sub-objective function fluctuates slightly but has little effect, and the objective function F shows a downward trend. The example simulation analysis results indicate that the optimization effect of the TEU-BQCT model is better by increasing the working efficiency of the quay

Table 8
Comparative analysis results of TEU-BQCT model and existing model.

	TEU-BQCT	E-B&QC [18]	TEU-BQCT vs E-B&QC[18]
Time of vessels in port	12.87	12.07	6.66% increase
Truck carbon emissions	14,921.95	16,799.84	11.18% reduction
Quay crane's carbon emissions	15,573.20	20,198.67	22.90% reduction
Additional waiting time for the vessel	19.84	15.52	27.80% increase

crane.

2) Effect of the carbon emission coefficient of trucks.

Second, we set different carbon emission coefficients to test the effect of the change of the coefficient on the TEU-BQCT model. Fig. 6 exhibits the experimental results. Compared with the carbon emission coefficient of 2.45 kg/L, the objective function F increased by 2.82% and 6.31% respectively in the case of the coefficient of 2.65 kg/L and 2.85 kg/L.

The experimental results show that following the improvement of the carbon emission coefficient, the sub-objective functions F_1 and F_3 have little overall change, and the sub-objective function F_2 and the objective function F show a slight upward trend. All in all, the TEU-BQCT model can still guarantee its optimization effect when the carbon emission

Table 9
Comparison algorithm parameter selection.

Swarm intelligence optimization algorithm			
Algorithm name	Total group number	The maximum number of iterations	Other additional hyperparameters
HHO[59]	50	100	—
SOA[3]	50	100	$f_c = 2$, $p_m = 0.10$
ASOA	50	100	$f_c = 2$, $p_m = 0.10$
Csoa	50	100	$f_c = 2$, $p_m = 0.10$
QSOA	50	100	$f_c = 2$, $p_m = 0.10$
CQASOA	50	100	$f_c = 2$, $p_m = 0.10$
Other optimization algorithms			
Algorithm name	Algorithmic hyperparameters		
SASS[56]	$N = 100$, $H = 50$		
COLSHADE [57]	$N_{\min} = 4$, $q_0 = 0.5$, $M_{CR} = 0.5$, $M_F = 0.5$, $M_{CRL} = 0.5$, $M_{FL} = 0.5$		
sCMAGES[58]	$P_\sigma = 0$, $P_c = 0$, $C^0 = 0$, $FE_{\max} = 100$		

coefficient changes.

3) Effect of the port size.

Finally, we test the effect of port size on the TEU-BQCT model based on data from two scale ports in Section 5.1. Fig. 7 exhibits the example simulation analysis results. In Fig. 7, we can find that the effect achieved by the TEU-BQCT model when applied to large ports (reducing the vessel's turnaround time, the carbon emissions of trucks, and the carbon emissions of quay cranes by 19.74%, 24.47%, and 17.80%) is better than that achieved when applied to small ports (reducing the vessels

turnaround time, the carbon emissions of trucks, and the carbon emissions of quay cranes by 12.46%, 19.11%, and 9.88%).

The comparative analysis results show that the TEU-BQCT model can adapt to different ports and provide corresponding scheduling schemes. Also, the optimization effect is more obvious as the port scale increases.

5.2.3. Comparative analysis with existing models

Aiming at testing the model performance, we selected the comparative model in the literature [18] for comparative analysis. The vessel's turnaround time, the additional transport distance cost of the container trucks and the additional waiting time cost for vessels are defined as the objective functions of the E-B&QC model. Thus, according to the solution results, we convert the extra truck transport cost into the carbon emission of the truck. The vessel turnaround time, the carbon emission from the container truck, the carbon emission from the quay crane, and the extra waiting time of the vessel are defined as comparative analyses of technical indicators. Table 8 shows the calculation results.

In Table 8, the results have the same effect in lowering vessel turnaround time, with a difference of only 6.66% solved by applying the TEU-BQCT model and the comparative model. Compared with the comparative model, the dispatching scheme obtained by applying the TEU-BQCT model can be reduced by 11.18% and 22.90%, respectively, in terms of reducing carbon emissions from trucks and quayside cranes, which indicates that the port application of TEU-BQCT model can obtain a solution to reduce carbon emissions. The additional waiting time of the scheduling scheme is increased by 27.80% by applying the TEU-BQCT model. However, various factors such as berths, quay cranes, and trucks are thought over in the TEU-BQCT model which will inevitably increase the time. In contrast, the comparative model is too ideal, and the additional waiting time of vessels is used as the objective function, so a scheduling scheme with a lower additional waiting time of vessels will

Table 10
Calculation results of 9 algorithms of the 1–5 times when solving the TEU-BQCT model.

100 Iteration Experience	1	2	3	4	5
Vessels turnaround time F_1	SASS[56] 11.83	11.27	11.93	10.28	11.26
	COLSHADE[57] 12.37	13.87	14.57	10.96	10.15
	sCMAGES[58] 14.28	14.03	13.93	13.73	12.83
	HHO[59] 10.73	10.67	12.93	15.03	10.97
	SOA[3] 11.85	13.16	13.78	12.96	12.69
	ASOA 12.32	12.56	11.71	10.85	10.61
	Csoa 13.65	10.74	10.29	11.08	11.43
	QSOA 10.25	11.70	11.83	9.86	10.83
	CQASOA 10.56	9.88	9.62	11.02	11.05
Truck carbon emissions F_2	SASS[56] 14,601.61	14,763.29	14,729.28	15,107.35	14,609.79
	COLSHADE[57] 14,829.28	13,972.27	14,829.29	14,527.29	14,827.29
	sCMAGES[58] 14,672.28	14,820.12	14,682.38	15,032.28	14,892.37
	HHO[59] 14,829.38	14,729.28	15,272.27	14,682.28	14,872.27
	SOA[3] 14,436.56	14,534.22	14,373.51	15,288.95	14,581.79
	ASOA 14,784.66	14,357.11	14,974.99	15,102.34	14,718.44
	Csoa 15,451.96	15,760.95	14,432.79	14,823.97	14,376.70
	QSOA 14,685.43	14,692.03	15,383.85	14,381.43	14,629.20
	CQASOA 14,018.24	15,009.87	15,411.47	14,665.62	14,311.81
Quay crane carbon emissions F_3	SASS[56] 17,624.27	17,682.39	16,293.29	17,654.57	16,982.28
	COLSHADE[57] 17,362.28	18,272.28	16,829.29	16,928.38	16,293.27
	sCMAGES[58] 17,292.39	17,928.22	18,273.29	17,928.38	18,392.47
	HHO[59] 16,832.35	18,272.37	18,682.27	20,834.27	21,829.38
	SOA[3] 16,300.83	17,671.85	17,453.81	17,024.90	16,907.91
	ASOA 16,469.93	16,403.40	18,180.37	18,157.74	16,306.28
	Csoa 17,968.48	19,161.64	17,802.03	17,313.07	17,447.88
	QSOA 16,891.00	16,845.06	18,185.71	16,671.49	16,101.31
	CQASOA 16,388.48	16,798.23	17,428.64	16,371.71	15,955.23
Objective function F	SASS[56] 13,971.07	13,747.76	13,719.78	13,331.94	13,528.02
	COLSHADE[57] 14,234.84	14,997.55	15,201.11	13,345.87	12,852.99
	sCMAGES[58] 15,132.27	15,201.23	15,203.02	15,104.31	14,735.82
	HHO[59] 13,279.54	13,586.88	14,952.27	16,393.28	14,661.72
	SOA[3] 13,608.81	14,631.35	14,846.48	14,559.03	14,216.28
	ASOA 13,971.52	13,969.73	14,146.05	13,740.34	14,485.24
	Csoa 15,181.84	14,099.92	13,204.66	15,131.71	13,671.20
	QSOA 13,021.23	13,733.74	14,307.77	12,691.92	13,100.09
	CQASOA 12,880.85	12,891.85	13,021.25	13,267.17	13,091.09

Table 11

Calculation results of 9 algorithms of the 6–10 times when solving the TEU-BQCT model.

100 Iteration Experience	6	7	8	9	10
Vessels turnaround time F_1	SASS[56]	10.98	11.98	10.38	10.95
	COLSHADE[57]	11.73	11.93	11.73	14.83
	sCMAgES[58]	14.27	11.63	13.87	13.83
	HHO[59]	12.54	14.27	13.73	14.73
	SOA[3]	13.72	11.33	14.24	10.42
	ASOA	11.60	11.30	12.53	10.42
	CSOA	11.44	11.98	14.12	14.64
	QSOA	15.34	10.81	10.55	11.13
	CQASOA	10.18	9.47	11.45	10.04
Truck carbon emissions F_2	SASS[56]	14,682.84	14,293.12	14,653.27	14,218.80
	COLSHADE[57]	14,382.28	14,521.39	14,392.28	13,892.28
	sCMAgES[58]	14,982.28	14,829.23	14,923.23	14,724.28
	HHO[59]	14,983.23	14,729.28	15,103.28	15,029.27
	SOA[3]	14,491.29	15,017.58	15,075.01	13,965.84
	ASOA	15,100.94	15,053.74	15,306.29	14,625.89
	CSOA	14,083.00	14,211.90	14,627.94	14,559.43
	QSOA	14,453.58	14,941.44	14,576.72	14,534.35
	CQASOA	14,331.86	14,361.52	14,670.70	14,987.24
Quay crane carbon emissions F_3	SASS[56]	17,679.90	17,839.28	18,273.28	19,372.48
	COLSHADE[57]	16,938.22	18,262.39	17,282.38	18,262.28
	sCMAgES[58]	17,292.29	19,837.28	18,273.29	19,273.27
	HHO[59]	20,182.38	19,234.28	19,823.28	20,321.28
	SOA[3]	21,301.37	15,751.42	22,958.85	17,345.66
	ASOA	17,477.80	17,891.25	18,008.81	16,205.53
	CSOA	16,416.62	17,041.45	16,999.76	21,609.60
	QSOA	21,409.89	17,532.98	16,441.06	19,071.61
	CQASOA	16,511.59	16,779.30	15,622.09	16,923.47
Objective function F	SASS[56]	13,578.52	14,025.50	13,423.10	13,872.82
	COLSHADE[57]	13,694.27	14,160.31	13,783.32	15,453.28
	sCMAgES[58]	15,205.10	14,480.77	15,235.59	15,414.03
	HHO[59]	15,060.09	15,627.31	15,595.79	14,202.24
	SOA[3]	15,805.80	13,356.30	16,629.36	14,769.01
	ASOA	13,945.32	13,886.34	14,594.45	14,365.14
	CSOA	13,347.38	13,801.00	14,966.89	16,362.88
	QSOA	16,635.36	13,522.36	13,031.43	15,952.06
	CQASOA	12,801.89	12,521.59	13,298.58	12,999.28

Table 12

The average result of the objective function in solving the TEU-BQCT model.

100 Iteration Experience	Vessels turnaround time F_1	Truck carbon emissions F_2	Quay crane carbon emissions F_3	Objective function F
SASS[56]	11.13	14,603.45	17,867.40	13,683.90
COLSHADE [57]	12.31	14,420.30	17,372.32	14,104.72
sCMAgES[58]	13.57	14,878.87	18,370.34	15,095.93
HHO[59]	12.63	15,051.29	19,638.42	14,988.69
SOA[3]	12.44	14,634.25	17,910.52	14,682.45
ASOA	11.47	14,929.87	17,184.14	14,198.32
CSOA	12.03	14,708.14	17,878.05	14,319.62
QSOA	11.36	14,699.29	17,556.34	14,070.29
CQASOA	10.33	14662.78	16,499.74	12,953.81

be obtained.

In conclusion, compared with the comparison model, the TEU-BQCT model established in this paper can better obtain a scheduling scheme to reduce the time of ship in port, port cost and carbon emissions.

5.3. Performance analysis for the CQASOA

Considering the good performance of SASS [56], COLSHADE [57], sCMAgES [58], and HHO [59] in solving the single objective constrained optimization problems, they are selected to test the capability of solving the TEU-BQCT model with regard to the proposed CQASOA. Also, SOA [3], ASOA, CSOA, and QSOA are selected to test the effectiveness of algorithm improvements. The idea of control variables is adopted to select and compare the algorithm parameters, to avoid different effects of different algorithm parameters on the optimization performance.

Table 13

Stability analysis table of 9 algorithms in solving the TEU-BQCT model.

100 Iteration Experience	Objective function F			
	Maximum	Minimum	Average	Standard deviation
SASS[56]	14,025.50	13,331.94	13,683.90	216.66
COLSHADE[57]	15,453.28	12,852.99	14,104.72	828.40
sCMAgES[58]	15,414.03	14,480.77	15,095.93	262.20
HHO[59]	16,527.78	13,279.54	14,988.69	1036.15
SOA[3]	16,629.36	13,356.30	14,682.45	911.70
ASOA	14,879.05	13,740.34	14,198.32	347.56
CSOA	16,362.88	13,204.66	14,319.62	985.72
QSOA	16,635.36	12,691.92	14,070.29	1265.58
CQASOA	13,298.58	12,521.59	12,953.81	223.02

Table 9 exhibits the parameters of the selected optimization algorithm.

5.3.1. Optimize performance analysis

The above algorithm is applied to solve the TEU-BQCT model 10 times in the case of large-scale ports. Table 10 and Table 11 show the calculation results:

The data in Table 10 and Table 11 is arranged, and the average of the solution results is calculated as exhibited in Table 12:

In Table 12, compared with SASS, COLSHADE, sCMAgES, and HHO, the value of objective function F can be reduced by 5.53%, 8.16%, 14.19%, and 13.58% via applying CQASOA to solve, indicating that CQASOA has the advantage of iterative update of spiral search and quantum local exploration, thus, its performance is better than traditional intelligent optimization algorithm when solving TEU-BQCT.

In comparison with SOA, the value of objective function F can be decreased by 3.30%, 2.47%, and 4.17% applying ASOA, CSOA, and

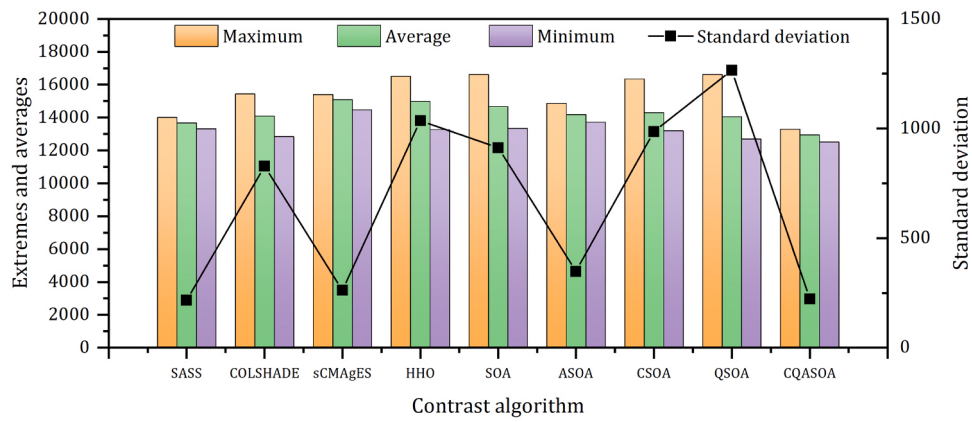


Fig. 8. Comparison chart of stability analysis of 9 algorithms for solving TEU-BQCT model.

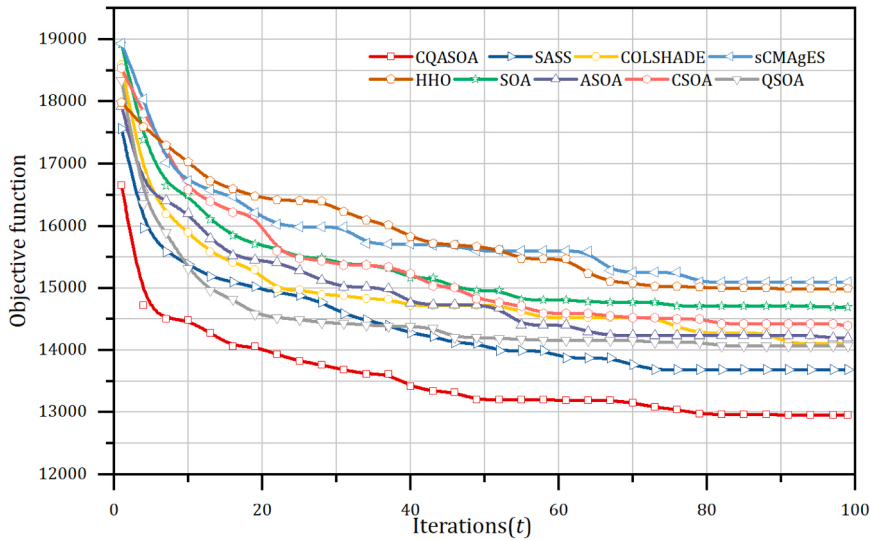


Fig. 9. 9 algorithms 10 times to calculate the average convergence curve.

QSOA, which illustrates that the algorithm optimization performance can be enhanced by adding the nonlinear weight, adding chaos disturbance and quantum computing; Contrasted to ASOA, CSOA, and QSOA, the objective function F can be cut down by 8.77%, 9.54%, and 7.94% through applying CQASOA to solve the problem, indicating that the CQASOA constructed by combining the three improved methods can get better results when solving the TEU-BQCT model.

5.3.2. Stability analysis

In view of the above data, the algorithm stability test is carried out, which reflects the quality of the solution when the algorithm solves the optimization problem many times. The calculation data in Table 10 and Table 11 is organized, the stability analysis table is shown in Table 13, and the stability analysis histogram is shown in Fig. 8:

In Table 13 and Fig. 8, the standard deviation of the CQASOA is close to the SASS and sCMAGES when solving the TEU-BQCT model, which indicates that the CQASOA is comparable to SASS and sCMAGES in terms of stability. Whereas, COLSHADE and HHO have higher standard deviations, whose stabilities are weaker than CQASOA.

The average solution value of ASOA is smaller than SOA, and the standard deviation is decreased by 61.88%, indicating that the expected purpose of improving the global disturbance ability in the early stage and increasing the local exploration ability in the later stage can be achieved by proposing the nonlinear convergence factor; There is little difference between applying SOA to solve variance and applying CSOA

to solve variance, but solving performance of CSOA is better than SOA, illustrating that the global exploration performance can be enhanced by adding chaotic disturbance in the initial stage of the population; Contrasted to SOA, the performance of QSOA with quantum computing is better than that of SOA, although the standard deviation is slightly larger than that of SOA, it is still within an acceptable range. In comparison with ASOA, CSOA, and QSOA, the mean is relatively optimal, and the standard deviation can be lowered by 35.83%, 77.37%, and 82.38% via using CQASOA to solve the TEU-BQCT model, showing that the fusion of the three improved methods is able to achieve the expected goal of raising the performance and stability of the algorithm.

5.3.3. Convergence analysis

Aiming at testing the algorithm convergence properties, this paper calculates the data based on Table 10 and Table 11, and draws the average convergence curve as shown in Fig. 9:

In Fig. 9, SOA has better convergence performance than SASS, COLSHADE, sCMAGES, and HHO, and has a strong continuous convergence ability. In comparison with SOA, the convergence performance of CSOA and ASOA is slightly better than SOA, and the convergence speed of QSOA is significantly better than SOA in the first 20 generations, illustrating that quantum improvement can speed up the convergence speed of SOA; The convergence performance of CQASOA is better than ASOA and CSOA, and slightly better than QSOA, which shows that the algorithm convergence performance can be enhanced by the fusion

improvement of linear convergence factor, chaotic disturbance, and quantum computing.

5.4. Practical applications and management implications

The purpose of constructing the TEU-BQCT_CQASOA solution method is to provide an effective decision-making aid for the intelligent dispatch of ports. The application of this method in actual dispatch can improve the economic, social, and environmental benefits. Its application value and importance mainly include the following aspects:

5.4.1. Trade-off

The TEU-BQCT_CQASOA solution method describes and solves the three conflicting objectives of the vessel time in port, the carbon emissions of trucks, and the carbon emissions of quay cranes. Port managers can weigh the advantages and disadvantages of each target according to the actual situation, adjust the weight adjustment coefficient of each target, and obtain a more suitable scheduling plan.

5.4.2. Shipowner and port interests

The TEU-BQCT_CQASOA solution method defines the vessel time in port as the objective function, which can raise the common interests of the vessel and the port. A good dispatch plan should ensure the economic benefits of the port as much as possible, and at the same time, it should improve the satisfaction of shipowners. Under the background of the post-epidemic era, it is even more necessary to apply the TEU-BQCT_CQASOA solution method to alleviate port congestion and improve port operation efficiency.

5.4.3. Green and low carbon

The TEU-BQCT_CQASOA solution method takes the carbon emissions of trucks and the carbon emissions of quay cranes as objective functions, which can provide port managers with a scheduling scheme to lower the carbon emissions of port working operations. In the context of the era of emphasis on reducing energy, smart ports need a solution that can not only ensure economic benefits but also ensure environmental benefits.

6. Conclusion

In response to the phenomenon of death congestion and slow operation in ports around the world in the post-epidemic era, this paper comprehensively considers the factors of tide, environment, and uncertainties and uses basic theories such as chaotic mapping, quantum computing, external penalty function method, and combines SOA to construct a novel berth-quay crane-truck joint scheduling solution (TEU-BQCT_CQASOA), which can supply an excellent scheduling scheme for container ports. The simulation examples of two container ports in South China show that the TEU-BQCT model can lessen vessels' turnaround time, the carbon emissions of trucks, and the carbon emissions from quay cranes, and as the scale of the port increases, a better dispatch plan can be obtained; Also, the TEU-BQCT model can satisfy the distinct demands of the port in different periods through the weight adjustment factor. The TEU-BQCT model established is based on the proposed CQASOA solution. When solving the TEU-BQCT model, CQASOA obtains a better solution compared with the comparative algorithm selected in this paper, and the solution process is more stable, more efficient, and more reliable.

However, the solution constructed in this paper still has inadequacy: many factors affect the scheduling of container ports, the model constructed in this paper will inevitably have ideal problems, and solutions need to be given in subsequent research; With the increase of the scale of the solving port, the dimension of the coding matrix increases and the solving process is complicated, which may make the increase of the time during the model solving process. In future research, follow-up research work on the problem of fast model solving is still needed.

Funding

The work is supported by the following project grants, National Natural Science Foundation of China (No.52371315); Heilongjiang Excellent Youth Fund Project (YQ2021E015); Science and Technology special fund of Hainan Province (ZDYF2023GXJS017); and National Council of Science and Technology, Taiwan (MOST 111–2410-H-161–001).

CRediT authorship contribution statement

Ming-Wei Li: Investigation, Methodology, Validation. Funding acquisition, Supervision, Writing- Original draft preparation. **Rui-Zhe Xu:** Conceptualization, Investigation, Methodology, Software, Data curation, Formal analysis, Validation. **Zhong-Yi Yang:** Conceptualization, Investigation, Software, Data curation, Formal analysis. **Wei-Chiang Hong:** Investigation, Methodology, Funding acquisition, Supervision, Writing- Reviewing, and Editing. **Xiao-Gang An:** Investigation, Methodology, Software, Data curation, Funding management. **Yi-Hsuan Yeh:** Software, Data curation, Formal analysis, Validation.

Declaration of Competing Interest

All authors claim that there's no financial/personal interest or belief that could affect their objectivity.

Data availability

Data will be made available on request.

References

- [1] G. Ye, J. Zhou, W. Yin, X. Feng, Are shore power and emission control area policies always effective together for pollutant emission reduction? – an analysis of their joint impacts at the post-pandemic era, *Ocean Coast. Manag.* 224 (2022) 106182, <https://doi.org/10.1016/j.ocecoaman.2022.106182>.
- [2] M.-M. Lu, Are ports still congested around the world? *Pearl River Water Transport* 4 (2022), 45–47. [In Chinese] <https://doi.org/10.14125/j.cnki.zjsy.2022.04.013>.
- [3] G. Dhiman, V. Kumar, Seagull optimization algorithm: theory and its applications for large-scale industrial engineering problems, *Knowl. -Based Syst.* 165 (2019) 169–196, <https://doi.org/10.1016/j.knosys.2018.11.024>.
- [4] A. Subramanian, J. Raman, Modified seagull optimization algorithm based MPPT for augmented performance of photovoltaic solar energy systems, *Automatika* 63 (2022) 1–15, <https://doi.org/10.1080/00051144.2021.1997253>.
- [5] J. Rupp, N. Boysen, D. Briskorn, Optimizing consolidation processes in hubs: the hub-arrival-departure problem, *Eur. J. Oper. Res.* 298 (2022) 1051–1066, <https://doi.org/10.1016/j.ejor.2021.07.001>.
- [6] C. Liang, X. Hu, L. Shi, H. Fu, D. Xu, Joint dispatch of shipment equipment considering underground container logistics, *Comput. Ind. Eng.* 165 (2022) 107874, <https://doi.org/10.1016/j.cie.2021.107874>.
- [7] H. Li, J. Peng, X. Wang, J. Wan, Integrated resource assignment and scheduling optimization with limited critical equipment constraints at an automated container terminal, *IEEE Trans. Intell. Transp. Syst.* 22 (2021) 7607–7618, <https://doi.org/10.1109/TITS.2020.3005854>.
- [8] J. Li, J. Yang, B. Xu, Y. Yang, F. Wen, H. Song, Hybrid scheduling for multi-equipment at u-shape trafficked automated terminal based on chaos particle swarm optimization, *J. Mar. Sci. Eng.* 9 (2021) 1080, <https://doi.org/10.3390/jmse9101080>.
- [9] H.-M. Fan, Z.-F. Guo, L.-J. Yue, M.-Z. Ma, Joint configuration and scheduling optimization of dual-trolley quay crane and AGV for container terminal with considering energy saving, *Acta Autom. Sin.* 47 (2021) 2412–2426, <https://doi.org/10.16383/j.ass.c190626>.
- [10] C. Bierwirth, F. Meisel, A survey of berth allocation and quay crane scheduling problems in container terminals, *Eur. J. Oper. Res.* 202 (2010) 615–627, <https://doi.org/10.1016/j.ejor.2009.05.031>.
- [11] C. Bierwirth, F. Meisel, A follow-up survey of berth allocation and quay crane scheduling problems in container terminals, *Eur. J. Oper. Res.* 244 (2015) 675–689, <https://doi.org/10.1016/j.ejor.2014.12.030>.
- [12] A. Liu, H. Liu, S.-B. Tsai, H. Lu, X. Zhang, J. Wang, Using a hybrid model on joint scheduling of berths and quay cranes-from a sustainable perspective, *Sustainability* 10 (2018) 1959, <https://doi.org/10.3390/su10061959>.
- [13] D. Ma, R. Zhang, X. Shao, 2018. Joint optimal scheduling of container terminal berths and quays based on improved cuckoo search, In: Proceedings of the 2018 International Conference on Computing and Data Engineering (ICCDE 2018), May 2018, pp. 103–109.<https://doi.org/10.1145/3219788.3219807>.

- [14] Z.-J. Gao, J.-X. Cao, Q.-Y. Zhao, Optimization research of berth allocation and quay crane assignment at container terminal based on the genetic algorithm, *Appl. Mech. Mater.* 505-506 (2014) 931–934, <https://doi.org/10.4028/www.scientific.net/AMM.505-506.931>.
- [15] J. Yu, G. Tang, X. Song, Collaboration of vessel speed optimization with berth allocation and quay crane assignment considering vessel service differentiation, *Transp. Res. Part E: Logist. Transp. Rev.* 160 (2022) 102651, <https://doi.org/10.1016/j.tre.2022.102651>.
- [16] W. Liu, X. Zhu, L. Wang, S. Li, Rolling horizon based robust optimization method of quayside operations in maritime container ports, *Ocean Eng.* 256 (2022) 111505, <https://doi.org/10.1016/j.oceaneng.2022.111505>.
- [17] M.-W. Li, W.-C. Hong, J. Geng, J. Wang, Berth and quay crane coordinated scheduling using multi-objective chaos cloud particle swarm optimization algorithm, *Neural Comput. Appl.* 28 (2017) 3163–3182, <https://doi.org/10.1007/s00521-016-2226-7>.
- [18] X. Cao, Z.-Y. Yang, W.-C. Hong, R.-Z. Xu, Y.-T. Wang, Optimizing berth-quay crane allocation considering economic factors using chaotic quantum SSA, *Appl. Artif. Intell.* 36 (2022) 2073719, <https://doi.org/10.1080/08839514.2022.2073719>.
- [19] A. Azab, H. Morita, The block relocation problem with appointment scheduling, *Eur. J. Oper. Res.* 297 (2022) 680–694, <https://doi.org/10.1016/j.ejor.2021.06.007>.
- [20] F. Essghaier, T. Chargui, T. Hsu, A. Bekrar, H. Allaoui, D. Trentesaux, G. Goncalves, Fuzzy multi-objective truck scheduling in multi-modal rail-road physical internet hubs, *Comput. Ind. Eng.* 182 (2023), <https://doi.org/10.1016/j.cie.2023.109404>.
- [21] J. Duan, Y. Liu, Q. Zhang, J. Qin, Combined configuration of container terminal berth and quay crane considering carbon cost, *Math. Probl. Eng.* 2021 (2021) 6043846, <https://doi.org/10.1155/2021/6043846>.
- [22] T. Wang, X. Wang, Q. Meng, Joint berth allocation and quay crane assignment under different carbon taxation policies, *Transp. Res. Part B: Methodol.* 117 (2018) 18–36, <https://doi.org/10.1016/j.trb.2018.08.012>.
- [23] N. Kenan, A. Jebali, A. Diabat, The integrated quay crane assignment and scheduling problems with carbon emissions considerations, *Comput. Ind. Eng.* 165 (2022) 107734, <https://doi.org/10.1016/j.cie.2021.107734>.
- [24] X. Tian, Q. Meng, Study on coordinated scheduling of berths, quay cranes and harbor trucks at container terminals, *Logist. Technol.* 37 (2018) 32–36, <https://doi.org/10.3969/j.issn.1005-152X.2018.03.008>.
- [25] N. Cheimanoff, F. Fontane, M.N. Kitri, N. Tchernev, . Exact and heuristic methods for the integrated berth allocation and specific time-invariant quay crane assignment problems, *Comput. Oper. Res.* 141 (2022) 105695, <https://doi.org/10.1016/j.cor.2022.105695>.
- [26] T. Jonker, M.B. Duinkerken, N. Yorke-Smith, A. de Waal, R.R. Negendorn, Coordinated optimization of equipment operations in a container terminal, *Flex. Serv. Manuf. J.* 33 (2021) 281–311, <https://doi.org/10.1007/s10696-019-09366-3>.
- [27] X.-G. Jiao, F.-F. Zheng, Y.-F. Xu, M. Liu, Integrated continuous berth allocation and time-variant quay crane assignment under berth dredging in container terminal, *Oper. Res. Manag. Sci.* 29 (2021) 47–57 [In Chinese]. <http://www.jorms.net/CN/10.12005/orms.2020.0033>.
- [28] L.P. Prencipe, M. Marinelli, A novel mathematical formulation for solving the dynamic and discrete berth allocation problem by using the bee colony optimisation algorithm, *Appl. Intell.* 51 (2021) 4127–4142, <https://doi.org/10.1007/s10489-020-02062-y>.
- [29] A. Skaf, S. Lamrous, Z. Hammoudan, M.-A. Manier, Integrated quay crane and yard truck scheduling problem at port of Tripoli-Lebanon, *Comput. Ind. Eng.* 159 (2021) 107448, <https://doi.org/10.1016/j.cie.2021.107448>.
- [30] J.-H. Chu, J.-H. Li, C.-J. Wang, C. Chen, Integrated decision on route planning and speed scheduling of container liners considering emission control areas, *J. Transp. Syst. Eng. Inf. Technol.* 21 (2021) 230–238, <https://doi.org/10.16097/j.cnki.1009-6744.2021.04.028>.
- [31] R.-E. Precup, E.-L. Hedrea, R.-C. Roman, E.M. Petriu, A.-I. Szedlak-Stinean, C.-A. Bojan-Dragos, Experiment-based approach to teach optimization techniques, *IEEE Trans. Educ.* 64 (2) (2021), <https://doi.org/10.1109/TE.2020.3008878>.
- [32] I. Alexandru Zamfirache, R.-E. Precup, R.-C. Roman, E.M. Petriu, Neural Network-based control using Actor-Critic reinforcement learning and Grey Wolf optimizer with experimental servo system validation, *Expert Syst. Appl.* 225 (2023), <https://doi.org/10.1016/j.eswa.2023.120112>.
- [33] R. Salgotra, S. Singh, U. Singh, S. Mirjalili, A.H. Gandomi, Marine predator inspired naked mole-rat algorithm for global optimization, *Expert Syst. Appl.* 212 (2023), <https://doi.org/10.1016/j.eswa.2022.118822>.
- [34] A.A. Ewees, R.R. Mostafa, R.M. Ghoniem, M.A. Gaheen, Improved seagull optimization algorithm using Lévy flight and mutation operator for feature selection, *Neural Comput. Appl.* 34 (2022) 7437–7472, <https://doi.org/10.1007/s00521-021-06751-8>.
- [35] B. Ma, P.-M. Lu, Y.-G. Liu, Q. Zhou, Y.-T. Hu, Shared seagull optimization algorithm with mutation operators for global optimization, *AIP Adv.* 11 (2021) 102517, <https://doi.org/10.1063/5.0073335>.
- [36] D. Xiao, L. Wan, Remote sensing inversion of saline and alkaline land based on an improved seagull optimization algorithm and the two-hidden-layer extreme learning machine, *Nat. Resour. Res.* 30 (2021) 3795–3818, <https://doi.org/10.1007/s11053-021-09876-8>.
- [37] L. Xu, Y. Mo, Y. Lu, J. Li, Improved seagull optimization algorithm combined with an unequal division method to solve dynamic optimization problems, *Processes* 9 (2021) 1037, <https://doi.org/10.3390/pr09061037>.
- [38] W.-C. Hong, M.-W. Li, J. Geng, Z. Yang, Novel chaotic bat algorithm for forecasting complex motion of floating platforms, *Appl. Math. Model.* 72 (2019) 425–443, <https://doi.org/10.1016/j.apm.2019.03.031>.
- [39] H.G. Kang, M.W. Li, P.F. Zhou, Z.H. Zhao, Prediction of passenger traffic volume using v-support vector regression optimized by chaos adaptive genetic algorithm, *J. Dalian Univ. Technol.* 52 (2012) 227–232, <https://kns.cnki.net/kcms/detail/detail.aspx?dbcode=CJFD&dbname=CJFD2012&filename=DLTG201202013&uniplatform=NZKPT&v=E6a7CnqJlzGFujzuWeCont5GOHGj8bsD1P6YNRXd2NavWXeKogwyqPa7x6z3Ar>.
- [40] M.-W. Li, W.-C. Hong, H.-G. Kang, Urban traffic flow forecasting using Gauss–SVR with cat mapping, cloud model and PSO hybrid algorithm, *Neurocomputing* 99 (2013) 230–240, <https://doi.org/10.1016/j.neucom.2012.08.002>.
- [41] M.-W. Li, J. Geng, W.-C. Hong, L.-D. Zhang, Periodogram estimation based on LSSVR-CCPSO compensation for forecasting ship motion, *Nonlinear Dyn.* 97 (2019) 2579–2594, <https://doi.org/10.1007/s11071-019-05149-5>.
- [42] M.-W. Li, Y.-T. Wang, J. Geng, W.-C. Hong, Chaos cloud quantum bat hybrid optimization algorithm, *Nonlinear Dyn.* 103 (2021) 1167–1193, <https://doi.org/10.1007/s11071-020-06111-6>.
- [43] M.-W. Li, D.-Y. Xu, J. Geng, W.-C. Hong, A ship motion forecasting approach based on empirical mode decomposition method hybrid deep learning network and quantum butterfly optimization algorithm, *Nonlinear Dyn.* 107 (2022) 2447–2467, <https://doi.org/10.1007/s11071-021-07139-y>.
- [44] M.-W. Li, D.-Y. Xu, J. Geng, W.-C. Hong, A hybrid approach for forecasting ship motion using CNN–GRU–AM and GCWOA, *Appl. Soft Comput.* 114 (2022) 108084, <https://doi.org/10.1016/j.asoc.2021.108084>.
- [45] Y. Song, N. Wang, Optimization of berthing plan of container terminal based on time uncertainty, *J. Transp. Syst. Eng. Inf.* 20 (2020) 224–230, <https://doi.org/10.16097/j.cnki.1009-6744.2020.04.032>.
- [46] Q. Qin, Z. Zhou, H. Lu, S. Wang, Y. Han, Route optimization of water-rail intermodal transport trucks considering carbon emission cost, *China Water Transp.* 10 (2021) 109–111, <https://doi.org/10.13646/j.cnki.42-1395.u.2021.10.039>.
- [47] G.-L. Tang, M. Qin, X.-Y. Zhao, Y. Qi, X. Li, Effects of container trucks scheduling modes on carbon emission in container terminal, *Port. Waterw. Eng.* 6 (2019) 46–51, <https://doi.org/10.3969/j.issn.1002-4972.2019.06.008>.
- [48] G. Li, C. Zheng, H. Yang, Carbon price combination prediction model based on improved variational mode decomposition, *Energy Rep.* 8 (2022) 1644–1664, <https://doi.org/10.1016/j.egyr.2021.11.270>.
- [49] R. Ghafari, N. Mansouri, An efficient task scheduling based on seagull optimization algorithm for heterogeneous cloud computing platforms, *Int. J. Eng., Trans. B: Appl.* 35 (2022) 433–450, <https://doi.org/10.5829/ije.2022.35.02b.20>.
- [50] S. EldeSouky, W. Elshafai, H.E.D.H. Ahmed, F.E.A. ElSamie, Cancelable electrocardiogram biometric system based on chaotic encryption using three-dimensional logistic map for biometric-based cloud services, *Secur. Priv.* 5 (2022) e198, <https://doi.org/10.1002/SPY2.198>.
- [51] P.L. Leonardo, M.J. Ricardo, R.C. Enrique, P.C. Michael, J.R. Omar, V.M. Rubén, Function composition from sine function and skew tent map and its application to pseudorandom number generators, *Appl. Sci.* 11 (2021) 5769, <https://doi.org/10.3390/APP11135769>.
- [52] Y. Dong, H.-M. Guo, Adaptive chaos particle swarm optimization based on colony fitness variance, *Appl. Res. Comput.* 28 (2011) 854–856, <https://doi.org/10.3969/j.issn.1001-3695.2011.03.015>.
- [53] S.-T. Xiang, D. Wang, Model interactive modification method based on improved quantum genetic algorithm, *J. Zhejiang Univ. (Eng. Sci.)* 56 (2022) 100–110, <https://doi.org/10.3785/j.issn.1008-973X.2022.01.011>.
- [54] D. Pizzocri, R. Genoni, F. Antonello, T. Barani, F. Cappia, 3D reconstruction of two-phase random heterogeneous material from 2D sections: An approach via genetic algorithms, *Nucl. Eng. Technol.* 53 (2021) 2968–2976, <https://doi.org/10.1016/J.NET.2021.03.012>.
- [55] N. Ab Aziz, H. Mid, Penalty function optimization in dual response surfaces based on decision maker's preference and its application to real data, *Symmetry* 14 (2022) 601, <https://doi.org/10.3390/sym14030601>.
- [56] Kumar A., Das S., Zelinka I. 2020a. A self-adaptive spherical search algorithm for real-world constrained optimization problems. In: GECCO 2020 Companion - Proceedings of the 2020 Genetic and Evolutionary Computation Conference Companion, 13–14. <https://doi.org/10.1145/3377929.3398186>.
- [57] Gurrola-Ramos J., Hernandez-Aguirre A., Dalmau-Cedeno O., 2020, COLSHADE for Real-World Single-Objective Constrained Optimization Problems. In: Proceedings of the 2020 IEEE Congress on Evolutionary Computation, CEC 2020 - Conference Proceedings. <https://doi.org/10.1109/CEC48606.2020.9185583>.
- [58] Kumar A., Das S., Zelinka I., 2020b, A modified covariance matrix adaptation evolution strategy for real-world constrained optimization problems. GECCO 2020 Companion - Proceedings of the 2020 Genetic and Evolutionary Computation Conference Companion, 11 - 12. <https://doi.org/10.1145/3377929.3398185>.
- [59] A.A. Heidari, S. Mirjalili, H. Faris, I. Aljarah, M. Mafarja, H. Chen, Harris hawks optimization: algorithm and applications, *Future Gener. Comput. Syst.* 97 (2019) 849–872, <https://doi.org/10.1016/j.future.2019.02.028>.